Report on distribution of rock modulus and correlation with temperature

D 5.11

Report on distribution of rock modulus and correlation with temperature

D 5.11

Version 10

Dimitrios Mendrinos, Spyros Karytsas and Constantine Karytsas (CRES);
Flavio Poletto, Biancamaria Farina (OGS)

Work package 5

25.11.2019

Website: http://www.gemex-h2020.eu

The GEMex project is supported by the European Union's Horizon 2020 programme for Research and Innovation under grant agreement No 727550

Table of Contents[1]

[1] The content of this report reflects only the authors' view. The Innovation and Networks Executive Agency (INEA) is not responsible for any use that may be made of the information it contains.

List of Figures

List of tables

Executive summary

Temperature measurements are available within geothermal wells down to circa 2 km depth or ~800 m asl elevation in Acoculco enhanced geothermal system (EGS), and down to circa 3 km depth or ~300 m bsl elevation in Los Humeros super-hot geothermal system. A constant temperature gradient is evident in Acoculco and a close to boiling-point-to-depth temperature pattern in Los Humeros.

In Acoculco EGS, one dimensional S-wave elastic modulus, calculated from ambient seismic noise analysis and local gravity survey, is related to measure temperature with a logarithmic function. This relationship may be also valid at deeper elevations below well bottom, down to the elevation where a local maximum elastic modulus is observed, as indicated when comparing S-wave modulus with extrapolated temperature calculated by the reservoir computer model of the field, which was developed within the GEMex project.

As an approximation, in Los Humeros super-hot geothermal system, P-wave elastic modulus, which was estimated from both legacy active and recent passive seismic 3-D surveys coupled to a regional gravity survey, increases almost linearly with depth down to 100m above sea level. S-wave elastic modulus, which was estimated by 1-D ambient seismic noise analysis and 3-D passive seismic survey coupled to a regional gravity survey, follows a similar pattern down to 500 m asl approximately, where its value stabilizes with depth. At deeper levels, S-wave modulus shows variations not shown by P-wave modulus.

In Los Humeros super-hot geothermal system, where 3-D data are available, seismic velocities and elastic moduli are correlated to temperature in the vertical direction by exponential functions, while no such statistically significant correlation is evident in the horizontal direction. This implies that an indirect relation may exist between seismic velocities and elastic moduli with temperature, e.g., through their dependence on common independent variables such as rock matrix pressure and/or pore pressure and fluid saturation. The weak correlations observed indicate that local anisotropy is also important.

1 Introduction

This deliverable is the result of the activities carried out for GEMex task 5.4.5 “Distribution of rock modulus of elasticity and correlation to temperature by comparing the spatial distribution of rock modulus of elasticity with the temperature distribution data derived from the thermo-mechanical models of task 3.3, as an effort to derive deep formation temperatures from seismic and gravity surveys”.

1.1 Objectives

The objectives of this work are:

- Evaluate formation temperatures in Los Humeros super-hot geothermal system and Acoculco EGS
- Estimate the P-wave modulus Ep and shear (S-wave) modulus Es from seismic and gravity surveys carried out in Los Humeros super-hot geothermal system and Acoculco EGS
- Investigate possible relationship between P-wave and S-wave seismic velocities with temperature
- Investigate possible relationship between P-wave and S-wave elastic moduli with temperature

1.2 Methodology

Evaluation of original formation temperature to depth (steady state, prior to drilling and testing in both Acoculco and Los Humeros and prior to energy production in Los Humeros) at the well locations in Los Humeros super-hot geothermal system and Acoculco EGS is performed using the following input data:

- P-T (Pressure and Temperature) logs provided by the Federal Electricity Commission of Mexico (CFE).
- Maximum recorded temperatures and static temperature projection using the Horner method, as provided by Damien Bonte (University of Utrecht), calculated for GEMex deliverable D3.4 “Regional resource assessment and geothermal models”.
- Static temperature projection using the Sphere method; Ref. Alfonso García Gutiérrez (2009), “Estado térmico inicial del campo geotérmico de Los Humeros, Puebla, México”, Geotermia, Vol. 22, No.1, Enero-Junio de 2009 (in Spanish).
- Temperature profiles at wells EAC-1 and EAC-2, as simulated by the reservoir models provided by Paromita Deb (RWTH-Aachen), developed for the GEMex deliverable D6.2 “Report on the numerical reservoir model used for the simulation of the Acoculco reservoir in Mexico”.
- Temperature profiles at selected wells, as simulated by the reservoir model provided by Paromita Deb (RWTH-Aachen), developed for the GEMex deliverable D6.3 “Report on the numerical reservoir model used for the simulation of the Los Humeros super-hot reservoir in Mexico”.

1-D and 3-D distribution to depth of formation P-wave and S-wave modulus is carried out by using the following equations:

$$E_p = \rho * V_p^2 \quad \text{and} \quad E_s = \rho * V_s^2 \qquad \text{(eq.1)}$$

where E_p and E_s are the P-wave and S-wave formation modulus respectively, ρ is the formation density and V_p and V_s are the P-wave and S-wave seismic velocities respectively.

Formation density distribution was taken from the output of the following formation density models:

- Local density models of Acoculco and Los Humeros provided by Dr. Natalia Cornejo (Karlruhe Institute of Technology - KIT) calculated from gravity survey carried out for GEMex deliverable D5.6 “Gravity modelling”.
- 3D regional density model from Los Humeros provided by the Mexican partners, obtained by joint inversion of gravity and magnetic methods assuming a direct relationship between density and magnetization (Marco A. Perez and Dr. Jonathan Carrillo Lopez, CICESE, Earth Sciences Division).

1-D and 3-D spatial distribution of seismic velocities was taken from the output of the following seismic velocity models:

- 1-D seismic velocity model of Acoculco provided by the Mexican partners (Dr. Marco Calo, Instituto de Geofísica, UNAM, PT5.2 SISMICA) calculated using ambient noise analysis.
- 1-D shear wave velocity profile of Los Humeros provided by Dr. Katrin Loeer (HS-Bochum), calculated from ambient seismic noise analysis for the GEMex Deliverable 5.3 on “Seismic structures of the Acoculco and Los Humeros geothermal fields”, chapter 5.7.
- 1-D Los Humeros seismic velocity model computation obtained from earthquake based travel-time tomography using the VELEST code, provided by Tania Andrea Toledo Zambrano (GFZ-Potsdam), developed for the GEMex deliverable D5.3 “Seismic structures of the Acoculco and Los Humeros geothermal fields”, chapter 5.4.
- 3-D Humeros seismic velocity model computation obtained from earthquake based travel-time tomography using the SIMUL2000 code, provided by Tania Andrea Toledo Zambrano (GFZ-Potsdam), developed for the GEMex deliverable D5.3 “Seismic structures of the Acoculco and Los Humeros geothermal fields”, chapter 5.4.
- Results from OGS processing of legacy active seismic raw data provided by CFE in the local model of the Los Humeros caldera Area (D5.3, Chapter 4).

In order to identify possible correlations between seismic velocities and elastic moduli with temperature using single or multiple variable regression analysis, theoretical models of seismic properties and trends were considered. These models included variation of elastic and viscoelastic moduli and velocities in geothermal systems with temperature under convective and conductive scenarios, as evaluated in GEMex deliverable D5.5 (D5.5, Annexes I and II).

Firstly, data interpolation, regression analysis, calculation of best fit trend lines and visualization were implemented with the MS-Excel software package. Using this methodology, two data files with seismic velocities, elastic moduli, density and temperature were created to be used as input to the SPSS 20 software package for further single and multiple variable statistical analyses. In both data files, values of Vp, Vs, Ep, Es, ρ and T were presented in arrays at well locations as a function of UTM coordinates X, Y and elevation Z; elevation Z was in increments of 100 m.

Data points selected for the analysis were all at well locations, because all available temperature data have been measured within the wells with high reliability, while temperature interpolation at locations between the wells adds additional errors due to the anisotropy of the subsurface, see also Figure 8 where many geological faults are evident in the Los Humeros superhot geothermal system.

The first data file included the values recently calculated by OGS for the Los Humeros active seismic survey of 1998 together with density and temperature as evaluated in Annex I, for each well at elevation increments of 100 meters and only for those elevation levels, where reliable estimates of temperature are available according to annex I. The second data file included the values calculated for the passive seismic survey carried out by the GEMex consortium during 2018, again together with density and temperature as evaluated in Annex I, for each well at elevation increments of 100 meters and only for those elevation levels, where reliable estimates of temperature are available according to annex I.

The 1998 data file comprised of 526 sets of data (total cases), referring to the year 1998. It included a) the name of the well, b) X, Y, Z coordinates, c) ρ (kg/m³) and, d) Vp (km/s) and Ep (kg/ms²) for each set. The 32 different wells taken into account are presented in Table 1.1, along with their X and Y coordinates and the data statistical frequency (number of data points) for each well.

The 2018 data file comprised of 698 sets of data (total cases), referring to the year 2018. It included a) the name of the well, b) X, Y, Z coordinates, c) ρ (kg/m³), d) Vp (km/s) and Ep (kg/ms²) and e) Vs (km/s) and Es (kg/ms²) for each set. The 45 different wells taken into account are presented in Table 1.2, along with their X and Y coordinates and the data statistical frequency (number of data points) for each well.

Once the data points were input in the statistical package SPSS 20, in addition to the exponential model between seismic velocities and elastic moduli with temperature, which has a theoretical basis and consistently yields among the highest R^2 values in the derived correlations, all 11 correlation functions provided by SPSS 20 as output were included in the analysis, as no additional effort was required.

Well	X	Y	Frequency (number of data points)	Percent of total data points
H-1	661906	2175064	18	3,4
H-10	662081	2176381	2	0,4
H-11	662574	2177436	23	4,4
H-13	662244	2174406	23	4,4
H-15	661638	2178804	19	3,6
H-16	661557	2178250	7	1,3
H-17	662298	2178606	7	1,3
H-19	662881	2176643	8	1,5
H-20	663330	2177486	23	4,4
H-21	662279	2179691	21	4,0
H-22	660055	2178853	3	0,6
H-26	663133	2175459	23	4,4
H-27	663986	2176292	10	1,9
H-29	661884	2177843	22	4,2
H-3	660622	2177903	17	3,2
H-30	661488	2178547	8	1,5
H-31	661832	2179041	19	3,6
H-32	662631	2178043	10	1,9
H-34	662965	2177207	18	3,4
H-37	661074	2178346	15	2,9
H-38	661897	2178155	22	4,2
H-40	661754	2175711	21	4,0
H-43	661240	2178060	22	4,2
H-45	661600	2176392	10	1,9
H-46	663021	2178288	19	3,6
H-48	662067	2175602	20	3,8
H-49	661866	2175003	20	3,8
H-55	663331	2177648	22	4,2
H-58	662555	2177456	22	4,2
H-7	661838	2175871	22	4,2
H-8	661582	2176392	22	4,2
H-9	660618	2178216	8	1,5

Table 1.1: Year 1998: wells under investigation, X and Y coordinates and corresponding data statistical frequency

Well	X	Y	Frequency (number of data points)	Percent of total data points
H-1	661906	2175064	18	2,6
H-10	662081	2176381	2	0,3
H-11	662574	2177436	23	3,3
H-12	663803	2173053	12	1,7
H-13	662244	2174406	23	3,3
H-13D	662364,1	2174569,405	3	0,4
H-14	663832	2169627	3	0,4
H-15	661638	2178804	19	2,7
H-16	661557	2178250	7	1,0
H-17	662298	2178606	7	1,0
H-18	664916	2172077	28	4,0
H-19	662881	2176643	8	1,1
H-2	662646	2172435	22	3,2
H-20	663330	2177486	23	3,3
H-21	662279	2179691	21	3,0
H-22	660055	2178853	3	0,4
H-23	664184	2175459	22	3,2
H-24	665497	2172938	8	1,1
H-25	666396	2176169	3	0,4
H-26	663133	2175459	23	3,3
H-27	663986	2176292	10	1,4
H-28	662601	2177741	3	0,4
H-3	660622	2177903	17	2,4
H-30	661488	2178547	8	1,1
H-31	661832	2179041	19	2,7
H-32	662631	2178043	10	1,4
H-33	661534	2177986	3	0,4
H-34	662965	2177207	18	2,6
H-37	661074	2178346	15	2,1
H-38	661897	2178155	22	3,2
H-39	663365	2173291	21	3,0
H-40	661754	2175711	21	3,0
H-42	663320	2173500	19	2,7
H-43	661240	2178060	22	3,2
H-45	661600	2176392	10	1,4
H-46	663021	2178288	19	2,7
H-48	662067	2175602	20	2,9
H-49	661866	2175003	20	2,9
H-50	663536	2173024	21	3,0
H-55	663330,4	2177648,236	22	3,2
H-58	662555	2177456	22	3,2
H-6	663508	2173545	24	3,4
H-7	661838	2175871	23	3,3
H-8	661582	2176392	23	3,3
H-9	660618	2178216	8	1,1

Table 1.2: Year 2018: wells under investigation, X and Y coordinates and corresponding data statistical frequency

Based on the above datasets, analyses were performed in order to investigate the relation between T and Vp, Ep, Vs and Es. It should be noted that for year 1998 dataset corresponding to the legacy active seismic survey, only Vp and Ep were examined – due to lack of available data on Vs and Es. Thus, the relation between T and Vp, Ep, Vs and Es was examined in the following contexts:

- Overall models examining the relation between T and Vp, Ep, Vs and Es, taking into account all different wells under examination, as presented in Table 1.1 for year 1998 and in Table 1.2 for year 2018.
- Overall models (i.e. taking into account all different wells under examination, as presented in Table 1.1 for year 1998 and in Table 1.2 for year 2018) examining the relation between T and the centred and normalized values of Vp, Ep, Vs and Es. For each one of these parameters Ω, its centred values were calculated as $(\Omega - \overline{\Omega_z})$, namely by subtracting its average value in the same elevation level; its normalized values were calculated as $(\Omega - \overline{\Omega_z}) / SD$, namely by diving the centred value by the standard deviation[2]. For the calculation of the standard deviation SD only the values corresponding to the horizontal layer under investigation were considered. In both cases, the average $\overline{\Omega_z}$ was estimated for each different level of elevation (Z).
- Individual model per well, meaning that the relation between T and Vp, Ep, Vs and Es was examined separately for each different well (i.e. keeping constant X and Y coordinates). The wells that were taken into account were those presented in Table 1.1 for year 1998 and Table 1.2 for year 2018; only wells with data (statistical) frequency ≥ 10 were taken into account, i.e., where at least 10 pairs of seismic velocities or elastic moduli and temperature are available.
- Individual model per elevation level (Z), meaning that the relation between T and Vp, Ep, Vs and Es was examined separately for each different elevation (i.e. keeping constant Z). The levels of elevation (Z) that were taken into account were those presented in Table 1.3 for year 1998 and Table 1.4 for year 2018; elevation levels (Z) with data (statistical) frequency ≥ 10 were taken into account.
- Overall models examining the relation between Z and Vp, Ep, Vs and Es, taking into account all different wells under examination, as presented in Table 1.1 for year 1998 and in Table 1.2 for year 2018.
- Multiple linear regression (MLR) models, taking into account all different wells under examination, as presented in Table 1.1 for year 1998 and in Table 1.2 for year 2018. Aim of the MLRs was to model the linear relationship between the explanatory (independent) variables (T and Z) and response (dependent) variable (Vp and Ep for year 1998; Vp, Ep, Vs and Es for year 2018).

For each one of the above cases different curves were estimated, including the following equations[3], where Ω is the dependent variable and T is the independent variable:

- ***Linear*.** Model whose equation is $\Omega = b_0 + (b_1 * T)$.
- ***Logarithmic*.** Model whose equation is $\Omega = b_0 + (b_1 * \ln(T))$.
- ***Inverse*.** Model whose equation is $\Omega = b_0 + (b_1 / T)$.

[2] SD: Standard Deviation; measure of the amount of variation of a set of values.
[3] https://www.ibm.com/support/knowledgecenter/en/SSLVMB_23.0.0/spss/base/curve_estimation_models.html

- ***Quadratic.*** Model whose equation is $\Omega = b_0 + (b_1 * T) + (b_2 * T^2)$.
- ***Cubic.*** Model that is defined by the equation $\Omega = b_0 + (b_1 * T) + (b_2 * T^2) + (b_3 * T^3)$.
- ***Power.*** Model whose equation is $\Omega = b_0 * (T^{b1})$ or $\ln(\Omega) = \ln(b_0) + (b_1 * \ln(T))$.
- ***Compound.*** Model whose equation is $\Omega = b_0 * (b_1 T)$ or $\ln(\Omega) = \ln(b_0) + (\ln(b_1) * T)$.
- ***S-curve.*** Model whose equation is $\Omega = e^{(b0 + (b1/T))}$ or $\ln(\Omega) = b_0 + (b_1/T)$.
- ***Logistic.*** Model whose equation is $\Omega = 1 / (1/u + (b_0 * (b_1^T)))$ or $\ln(1/\Omega - 1/u) = \ln(b_0) + (\ln(b_1) * T)$ where u is the upper boundary value.
- ***Growth.*** Model whose equation is $\Omega = e^{(b0 + (b1 * T))}$ or $\ln(\Omega) = b_0 + (b_1 * T)$.
- ***Exponential.*** Model whose equation is $\Omega = b_0 * (e^{(b1 * T)})$ or $\ln(\Omega) = \ln(b_0) + (b_1 * T)$.

Z, m	Frequency (number of data points)	Percent of total data points
300,00	1	0,2
400,00	1	0,2
500,00	7	1,3
600,00	15	2,9
700,00	18	3,4
800,00	21	4,0
900,00	25	4,8
1000,00	28	5,3
1100,00	28	5,3
1200,00	27	5,1
1300,00	27	5,1
1400,00	23	4,4
1500,00	22	4,2
1600,00	22	4,2
1700,00	22	4,2
1800,00	22	4,2
1900,00	22	4,2
2000,00	23	4,4
2100,00	23	4,4
2200,00	23	4,4
2300,00	23	4,4
2400,00	24	4,6
2500,00	24	4,6
2600,00	26	4,9
2700,00	29	5,5

Table 1.3: Year 1998: frequency of Z coordinates of the wells under investigation

Z, m	Frequency (number of data points)	Percent of total data points
-300,00	1	0,1
-200,00	1	0,1
-100,00	1	0,1
0,00	3	0,4
100,00	3	0,4
200,00	4	0,6
300,00	6	0,9
400,00	6	0,9
500,00	13	1,9
600,00	21	3,0
700,00	25	3,6
800,00	28	4,0
900,00	33	4,7
1000,00	35	5,0
1100,00	34	4,9
1200,00	33	4,7
1300,00	33	4,7
1400,00	30	4,3
1500,00	29	4,2
1600,00	29	4,2
1700,00	28	4,0
1800,00	28	4,0
1900,00	28	4,0
2000,00	29	4,2
2100,00	29	4,2
2200,00	29	4,2
2300,00	29	4,2
2400,00	28	4,0
2500,00	29	4,2
2600,00	29	4,2
2700,00	44	6,3

Table 1.4: Year 2018: frequency of Z coordinates of the wells under investigation

The resulting statistical models are presented in annexes 7-12, using the following symbols[4]:

- R Square (R^2): the curve fitting;
- F: the actual significance level of the check value;
- df1, df2: variance;
- Sig.: actual significance level of F;
- Constant: the absolute term (b0);
- b1, b2, b3: regression parameters of the curve.

[4] Liu, Z. L., Dong, X. F., Liu, Z. T., & Liu, Q. H. (Eds.). (2013). *Environmental Protection and Resources Exploitation*. Trans Tech Publications Ltd. pp 776.

1.3 Limitations

A main limitation is the accuracy and availability of reliable temperature estimates within the wells. This is because well tests and temperature measurements in the wells are usually designed in order to obtain information concerning the permeable zones, the production rates and the thermodynamic properties of the produced geothermal fluids and usually temperature logging is performed without allowing the well to rest for sufficient time, so that in-hole temperatures recover to their original values (before drilling and testing).

Specific limitations occurred during the analysis of both the overall models (i.e. including all wells) and the individual models (per well or per level of elevation (Z)). Specifically:

- Due to absence of shear velocity data, Vs and Es were not examined for year 1998 (Los Humeros CFE legacy active seismic survey), neither in overall nor in individual models.
- When referring to overall models examining the relation between level of elevation (Z) and Vp, Ep, Vs and Es, cases with $Z \leq 0$ have been excluded from overall models of year 2018 (Los Humeros passive seismic survey of GEMex consortium). This is due to the fact that when $Z = 0$ the inverse and S-curve models cannot be calculated; when $Z < 0$ the Logarithmic and Power models cannot be calculated.
- When referring to overall models –for both 1998 and 2018- examining the relation between T and the centred and normalized values of Vp, Ep, Vs and Es, cases with $\Omega - \overline{\Omega} = 0$ are not included in the presented models (thus reducing the number of total cases included in the overall models). In addition, in the occasions that $\Omega - \overline{\Omega}$ or $(\Omega - \overline{\Omega}) / SD$ contained non-positive values, the Compound, Power, S-curve, Growth, Exponential, and Logistic models were not calculated, as log transform could not be applied. The overall models facing this issue are mentioned in the "Notes" section in the beginning of each Annex.
- When referring to individual model per well, wells H-10, H-16, H-17, H-19, H-22, H-30 and H-9 for year 1998 (Table 1) and wells H-10, H-13D, H-14, H-16, H-17, H-19, H-22, H-24, H-25, H-28, H-30, H-33 and H-9 for year 2018 (Table 2) were not modelled, since they had a frequency < 10 cases.
- When referring to individual models per well for both 1998 and 2018, for specific wells the cubic and quadratic model could not be fitted due to near-collinearity among model terms; the wells facing this issue are mentioned in the "Notes" section in the beginning of each Annex.
- When referring to individual models per elevation level (Z), elevations of 300m, 400m and 500m a.s.l. for year 1998 (Table 3) and elevations of -300m, -200m, -100m, 0m, 100m, 200m, 300m and 400m a.s.l. for year 2018 (Table 4) were not modelled, since they had a frequency < 10 cases.
- When referring to individual models per elevation (Z) for both 1998 and 2018, at specific elevations the cubic model could not be fitted due to near-collinearity among model terms; the wells facing this issue are mentioned in the "Notes" section in the beginning of the corresponding Annex.
- When referring to individual models per elevation (Z) for both 1998 and 2018, models are not presented for wells where the independent variable (T) is a constant; the wells facing this issue are mentioned in the "Notes" section in the beginning of each Annex.

In Poletto et al. (2018) it is shown that relationships between seismic properties and temperature are not unique. This corresponds to very different geothermal scenarios, e.g., with and without rock melting. This condition could hold for the deep parts of Acoculco and Los Humeros.

The influence of pore pressure to the derived relationships of seismic velocities and elastic moduli with temperature has not been a subject of investigation in this work, as available pressure logs do not allow the estimation of pore pressure distribution in sufficient detail. The theoretical pressure effects to the trends of seismic velocities and rock moduli with temperature are shown in Poletto et al. (2018), where it is highlighted that in the upper porous fluid-saturated formations of a geothermal field, which is the case of the upper 3 km of Los Humeros and the upper 2 km of Acoculco investigated here, these trends are governed by pressure effects, with minor contributions of permeability and possible effects related to soft porosity.

1.4 Document structure

After the introduction where the objectives are presented, the methodology and the limitations of this work are described, the analysis is presented in each one geothermal field studied in separate chapters. For each geothermal field (Acoculco EGS and Los Humeros super-hot) the evaluation of temperature distribution, the estimation of formation moduli and the correlations derived, are presented in separate sub-chapters and a discussion of results follows. For the Los Humeros field, in each subchapter, the analysis and results are grouped according to the type of seismic survey considered.

Finally, the document includes the main conclusions derived, the references and the list of annexes.

The document is accompanied by thirteen annexes, which present the evaluation and processing of data used in this work. All annexes are confidential, as they include confidential data provided by CFE and unpublished research results provided by other members of the European and Mexican GEMex consortia, as mentioned in chapter 1.2.

2 Acoculco

2.1 Temperature distribution

The 1-D temperature distribution to depth in Acoculco enhanced geothermal system (EGS) is shown in Figure 1. Temperatures were calculated according to the evaluation presented in confidential Annex II. As in Acoculco only two geothermal wells have been drilled, a 3-D temperature model cannot be derived.

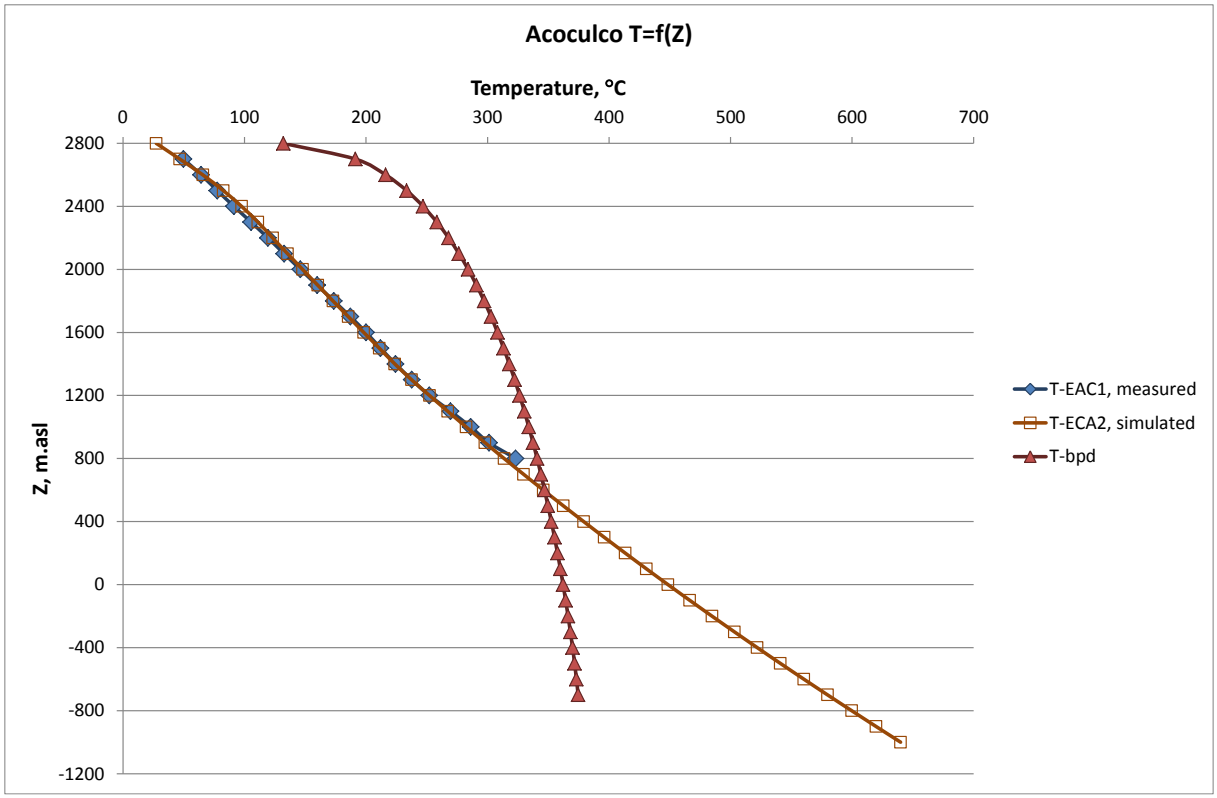

Figure 1: Steady state temperature profiles in Acoculco, as measured in well EAC-1 and as simulated by the reservoir model in well EAC-2 (provided by Dr. Paromita Deb, RWTH-Aachen), in comparison with the boiling point to depth (bpd) model.

Above temperature profile corresponds to conductive heat transfer model with constant temperature gradient, see Farina et al. 2019, indicating very low permeability, which is typical of EGS.

2.2 Formation Modulus

Using the one dimensional S-wave velocities calculated by the Mexican partners (Dr. Marco Calo, Instituto de Geofísica, UNAM, PT5.2 SISMICA) using ambient noise analysis, the rock densities at well sites EAC1 and EAC2 provided by Dr. Natalia Cornejo (Karlruhe Institute of Technology - KIT) calculated from gravity survey, the S-wave modulus Es in each well location was derived according to equation 1. The results are presented in Figure 2.

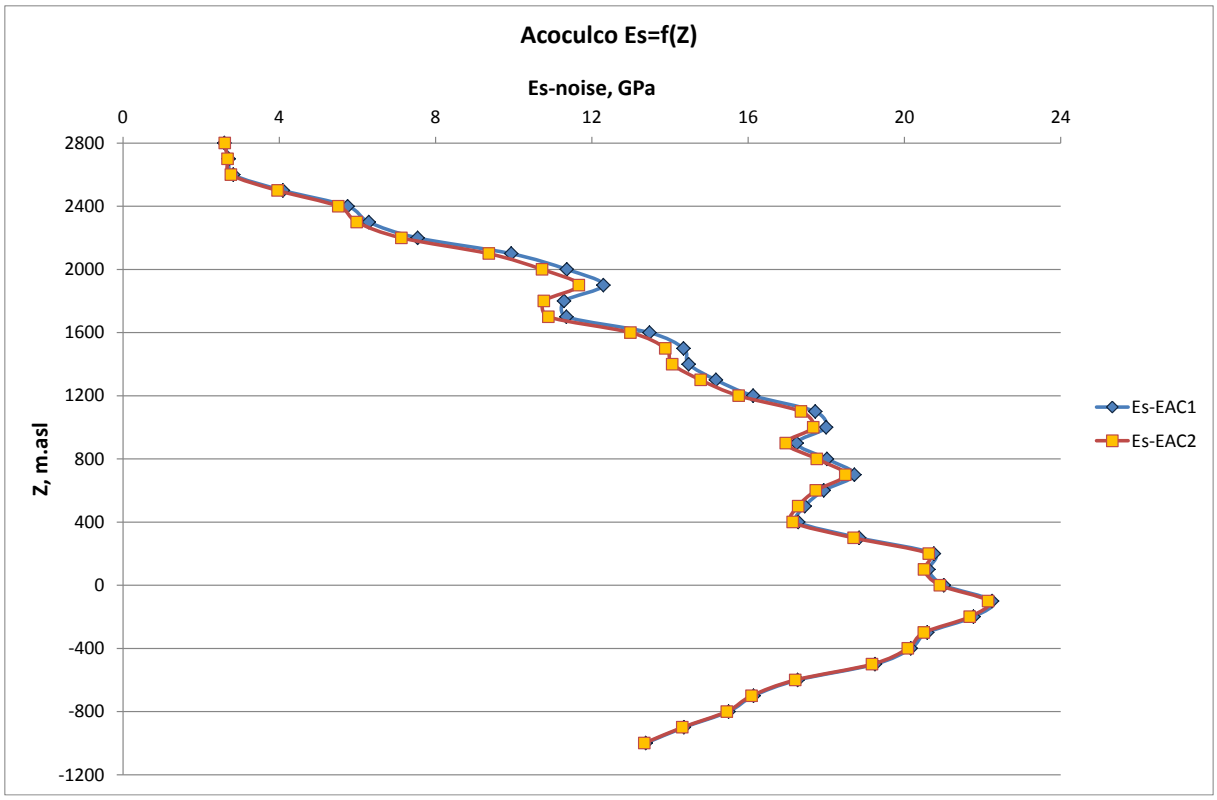

Figure 2: Profile of S-wave elastic modulus at the locations of wells EAC1 and EAC2 in Acoculco.

The values of Es at both well locations are approximately the same, as they have been calculated using the same 1-D Vs profile, which was the only one available for Acoculco geothermal field at the time of the preparation of this deliverable. The small differences observed at elevations from 2400 m asl down to 1000 m asl are attributed to the rock density variations in both locations.

2.3 Correlation to temperature

The graphs of S-wave velocity Vs and S-wave elastic modulus Es as a function to temperature for both measured (well EAC1) and simulated (EAC2) values are presented in Figures 3 and 4.

The correlation to temperature of both Vs and Es points to second order polynomial functions. The corresponding R^2 values are higher than 95%. However, different parameters are estimated as the corresponding constants, depending on whether measured or simulated temperature values are used for the calculation. Differences are more pronounced in the Vs case.

In the measured data of well EAC1, logarithmic functions of Vs=Vs(T) and Es=Es(T) can be also calculated as a best fit to data points, with corresponding R^2 values higher than 95%. However, the calculated logarithmic functions are also valid for the simulated data of EAC2 up to the maximum values of Vs and Es. These logarithmic functions based on EAC1 data seem to represent EAC2 data better in the case of Es, rather than in the case of Vs.

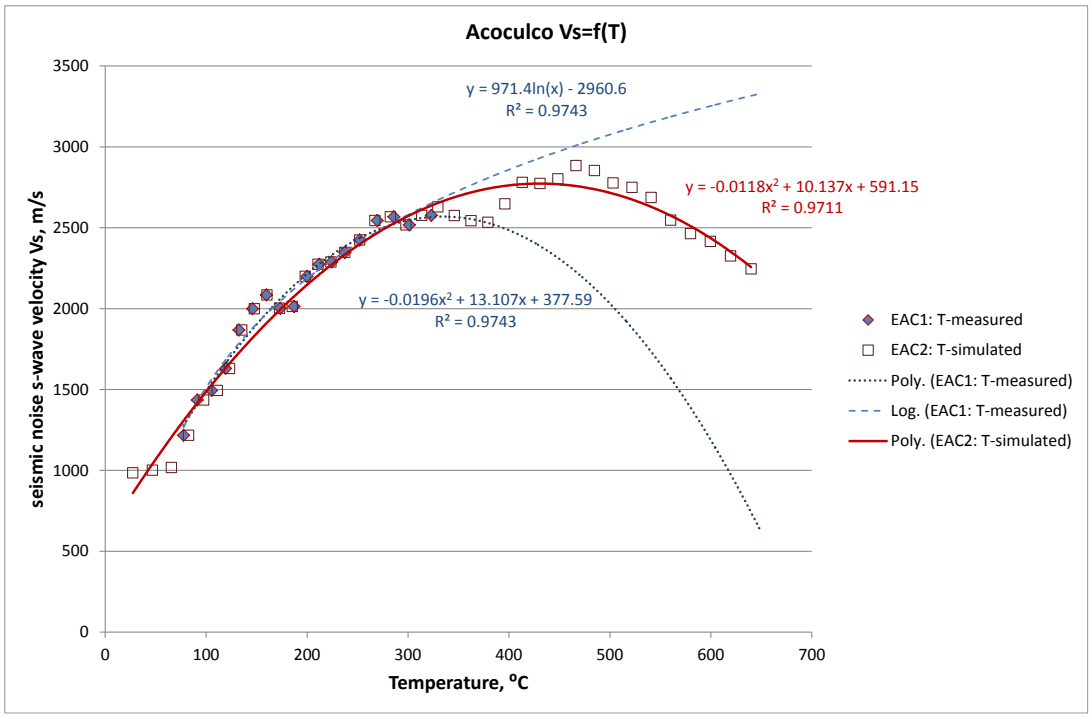

Figure 3: Relationships between S-wave velocity Vs with measured (EAC1) and simulated (EAC2) temperatures in Acoculco; for well EAC1 a best fit second order polynomial and a best fit logarithmic trendline have been calculated to available data, which correspond to measured values of both Vs and T; for EAC2 a second order polynomial trendline is presented as a best fit to data, which are measured values of Vs but simulated values of T.

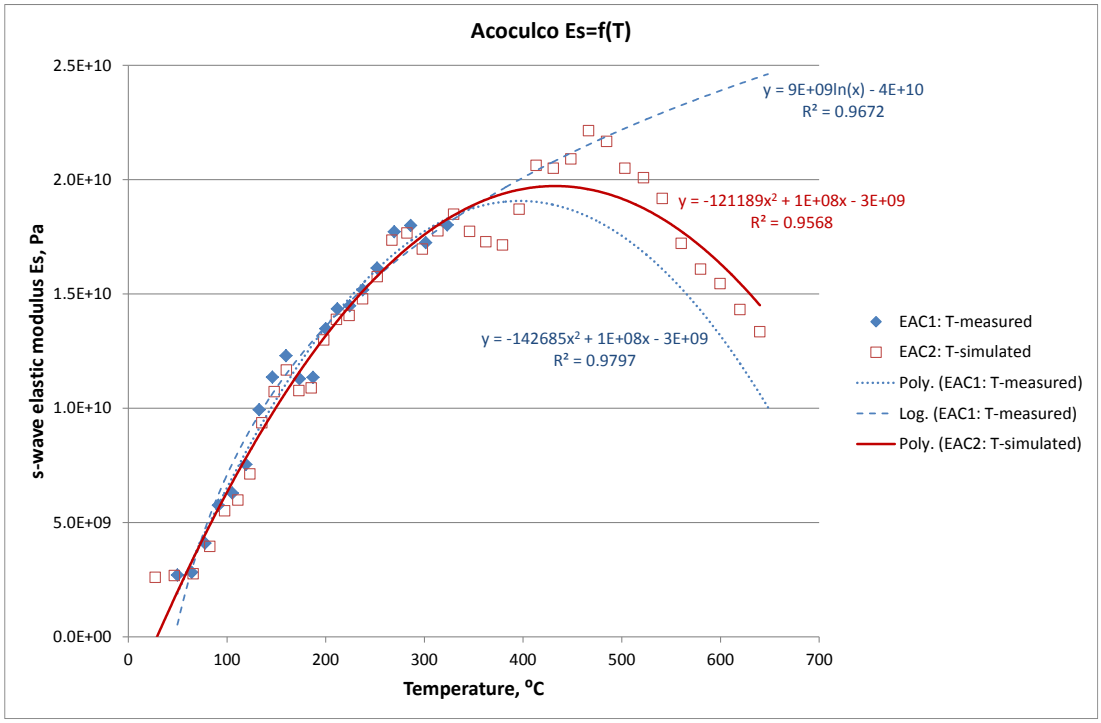

Figure 4: Relationships between S-wave elastic modulus Es with measured (EAC1) and simulated (EAC2) temperatures in Acoculco; for well EAC1 a best fit second order polynomial and a best fit logarithmic trendline have been calculated to available data, which correspond to measured values of both Vs and T; for EAC2 a second order polynomial trendline is presented as a best fit to data, which are measured values of Vs but simulated values of T.

2.4 Discussion

Inversion of the relationships presented in previous chapter in terms of temperature, is presented in Figure 5 for Vs and Figure 6 for Es. The best fit exponential function to measured data points is presented in each case (T vs Vs and T vs Es), with the corresponding R^2 being higher than 95%.

As expected from the analysis presented in previous chapter 2.3, the extrapolated exponential best fit also matches the simulated temperatures down to depth where the maximum Vs or Es were recorded, with the match being better in the case of Es, rather than Vs. This observation suggests that using the calculated exponential function presented in Figure 6 could provide hints for the temperature estimation at depths beneath the EAC1 well bottom. It is reminded that reliable steady state formation temperature measurements are available in the well EAC1, but no measured data are available below its well bottom.

The validity of the 1-D temperature prediction analysis presented here needs verification by measured rather than simulated temperature data, while its potential application in other geothermal fields needs further research in this direction.

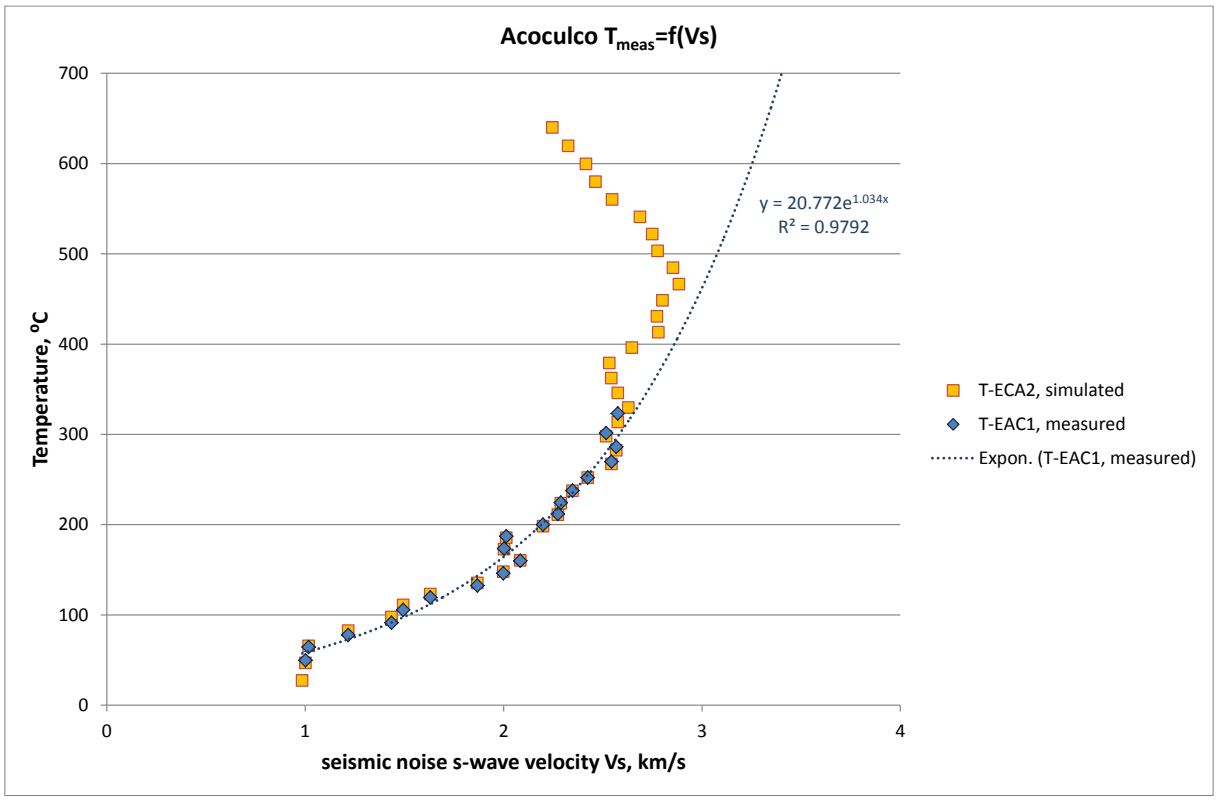

Figure 5: Measured and simulated temperature as a function of S-wave velocity in Acoculco and extrapolation of measured values using the best fit exponential function.

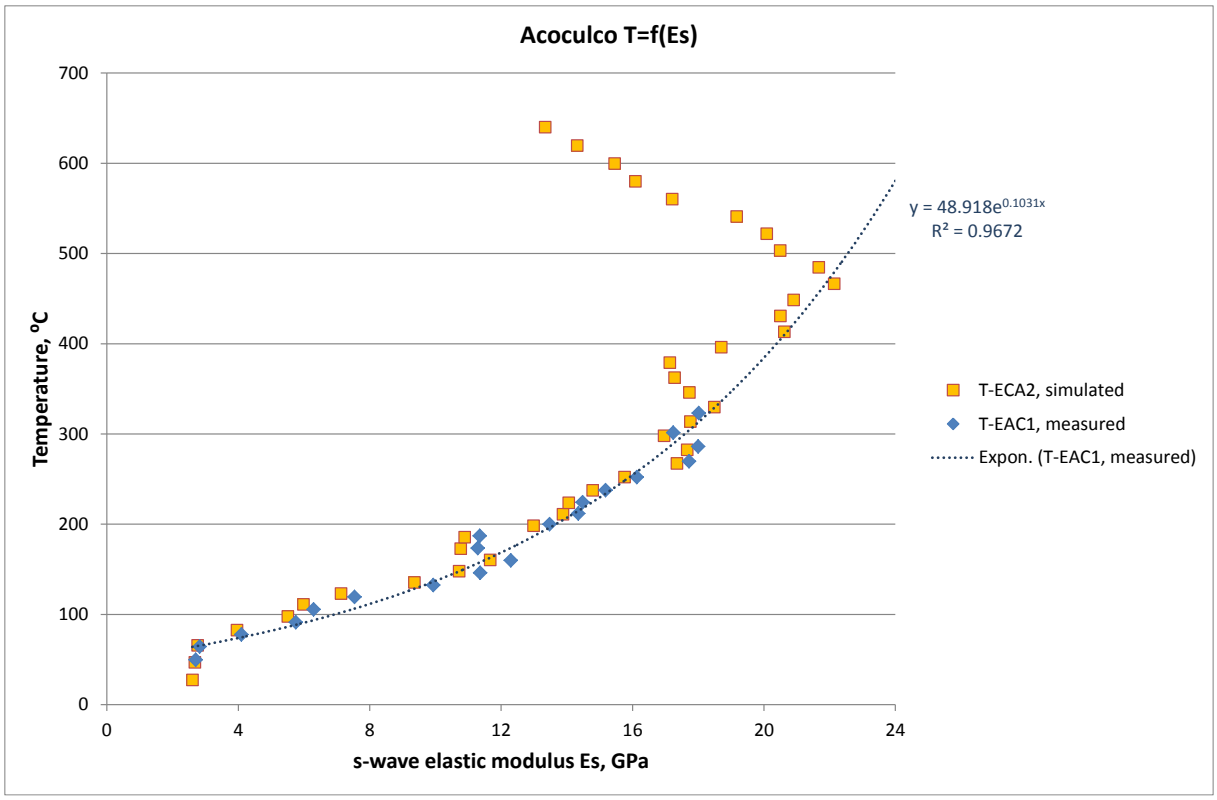

Figure 6: Measured and simulated temperature as a function of S-wave elastic modulus in Acoculco and extrapolation of measured values using the best fit exponential function.

3 Los Humeros

3.1 Temperature distribution

In Los Humeros geothermal field the temperature measurements in each one of the 52 wells drilled were evaluated in order to derive the steady state formation temperature. The evaluation is presented in confidential Annex I.

3.1.1. 1-D temperature distribution to depth

The steady state temperature distribution to depth in Los Humeros geothermal field is presented in Figure 7, where all reliable temperature values every 100 m of elevation in seep well are shown, in comparison to the boiling point to depth temperature model, which is typical for hydrothermal fields such as los Humeros. In the same Figure, the average temperature values are shown, which have been calculated by averaging all temperature values of the same elevation. The latter is considered as the one dimensional temperature (1-D T) of the Los Humeros field and is used in the 1-D analysis that follows.

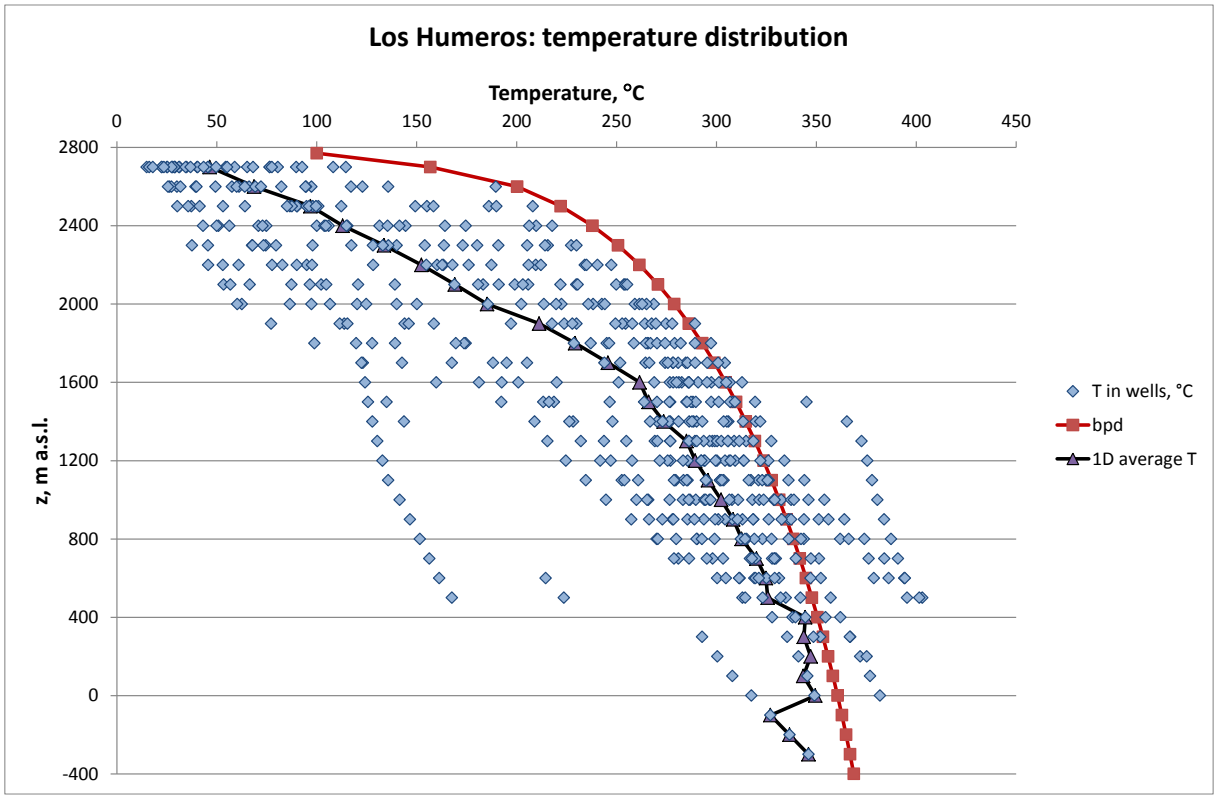

Figure 7: Temperature distribution to depth in Los Humeros geothermal field together with average values in each elevation level and the boiling point to depth (bpd) model.

3.1.2. 3-D temperature model

The steady state temperature model of Los Humeros, as derived from the evaluation of P-T logs in wells described in Annex I, is presented in Annex III in terms of horizontal cross sections. In this chapter, the above temperature model is summarized in terms of selected vertical cross sections, which are shown in Figures 9-11. In each cross section, the temperature at each pair of coordinates (X, Z) or (Y, Z) has been calculated using the XonGrid Interpolation Add-in of the MS-Excel. Interpolation method selected was Ordinary Kriging interpolation with the following parameters:

- method = 0: power variogram with exponent equal to 1,
- scaling = 0,
- SubKriging = 4: only the 4 nearest points are considered for the interpolation.

The locations of the Los Humeros wells used in the evaluation are shown in the map of Figure 8.

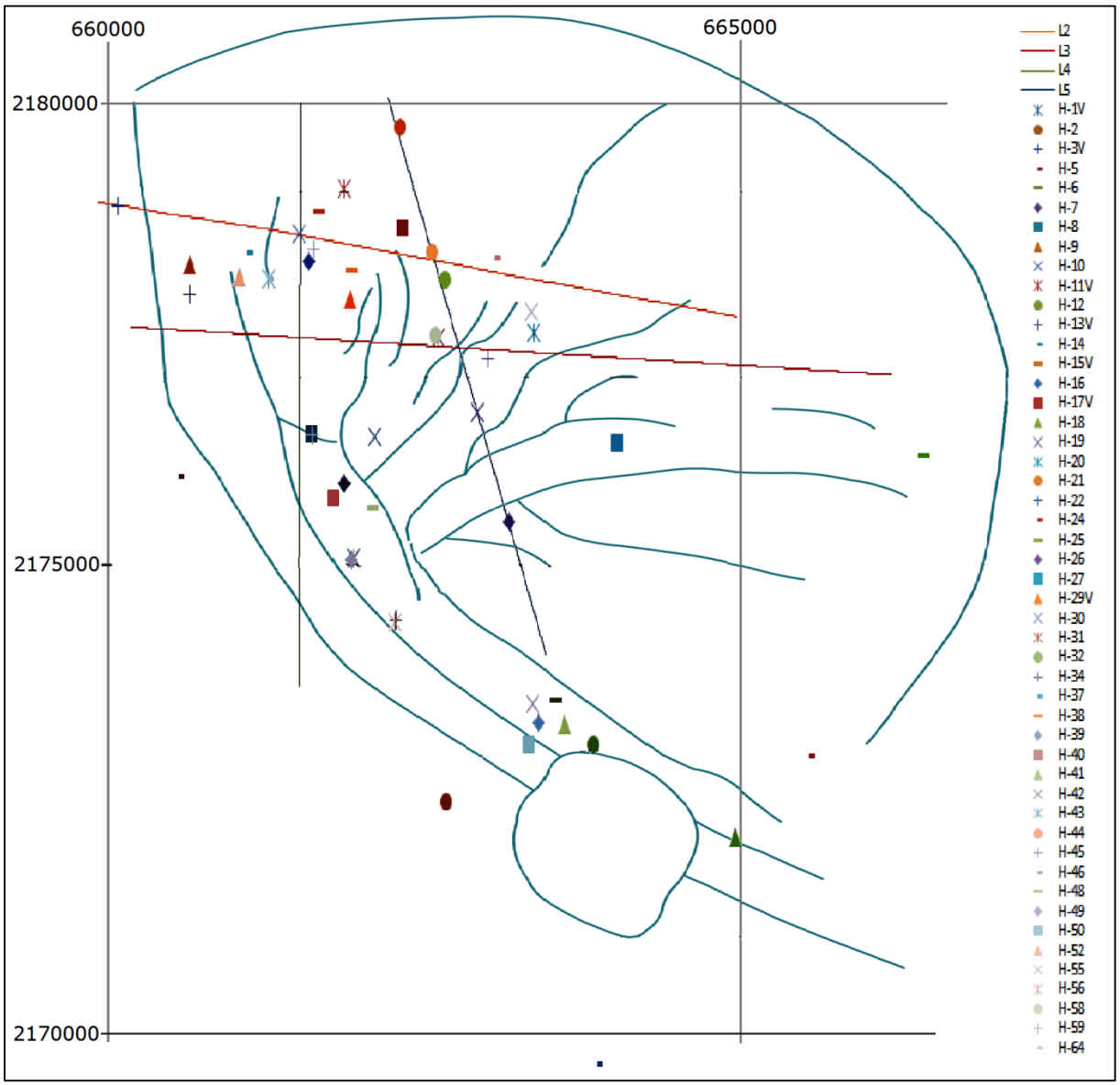

Figure 8: Well locations (H-n) and seismic lines (Ln) of the legacy CFE active seismic survey carried our during 1998, in comparison to main fault structures (green lines, see Calcagno et al. 2018) at Los Humeros in the UTM coordinate system.

Cross sections: vertical

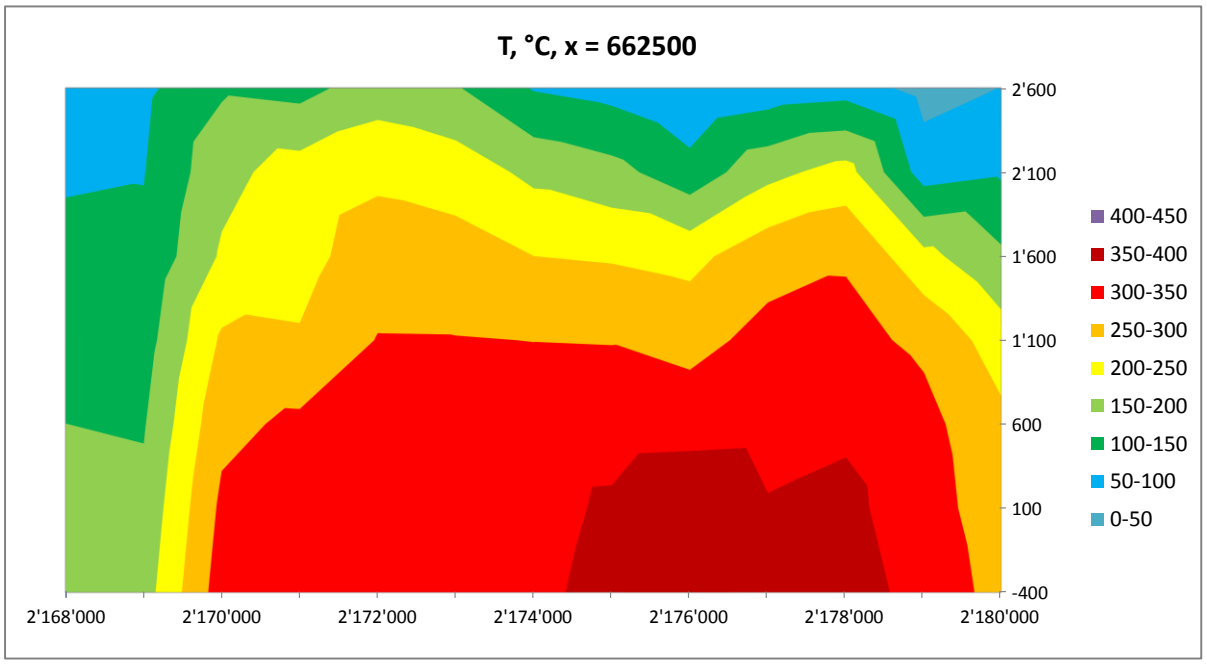

Figure 9: Temperature distribution along a vertical cross section of Los Humeros geothermal field in the direction South (left) – North (right) at x=662500 of the UTM coordinate system; the vertical axis corresponds to the z-coordinate in m.asl.

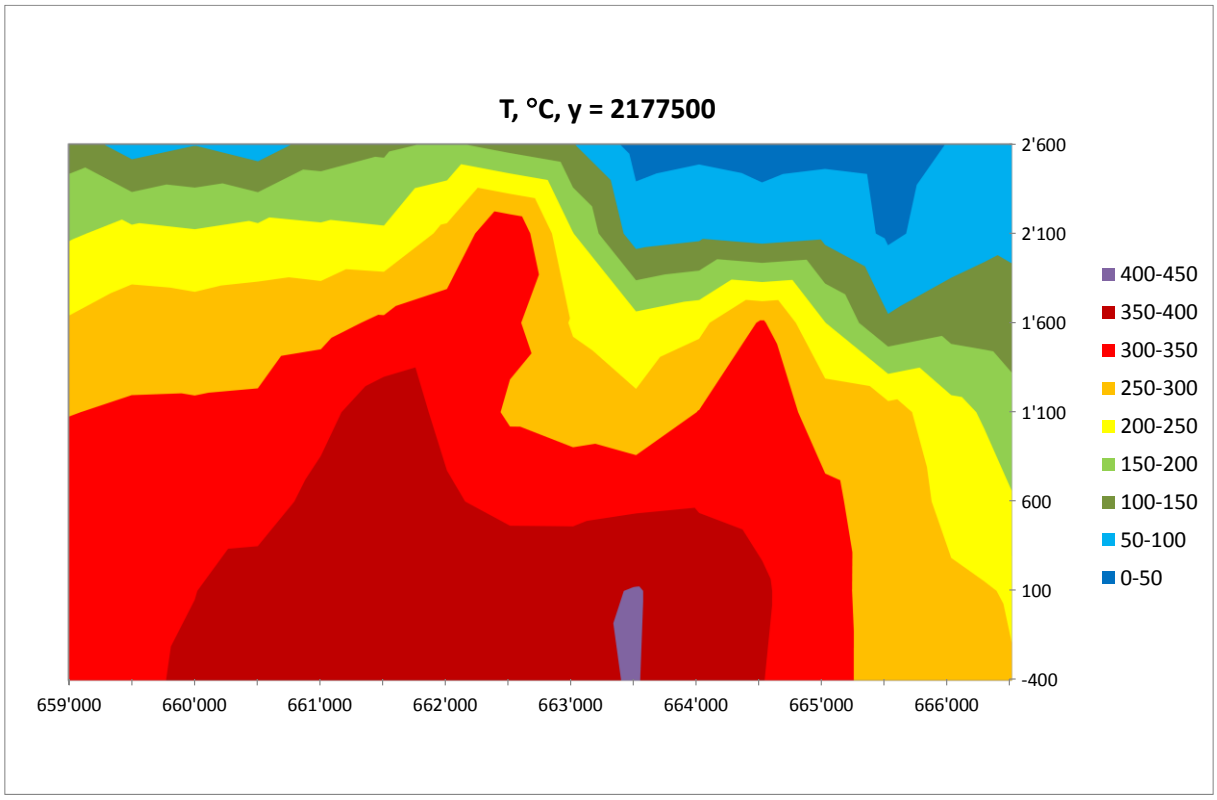

Figure 10: Temperature distribution along a vertical cross section of Los Humeros geothermal field in the direction East (left) -West (right) at y=2177500 of the UTM coordinate system; the vertical axis corresponds to the z-coordinate in m.asl.

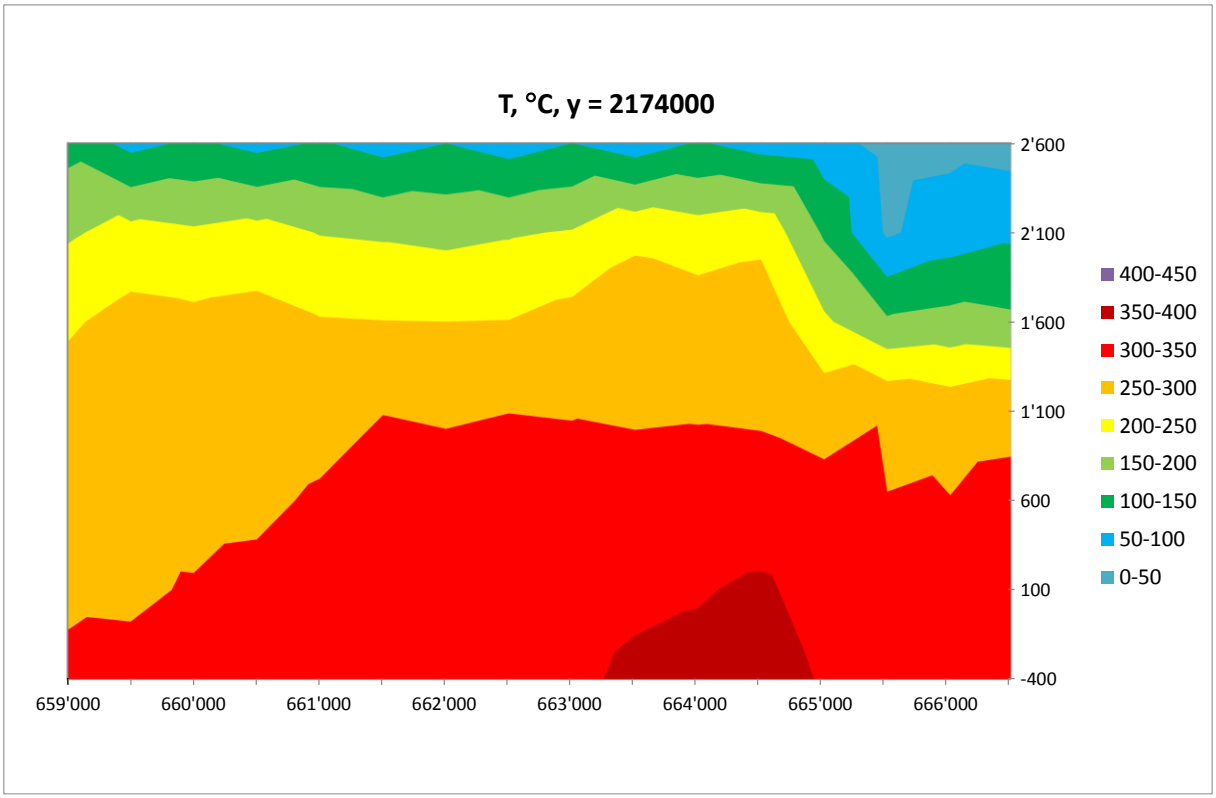

Figure 11: Temperature distribution along a vertical cross section of Los Humeros geothermal field in the direction East (left) -West (right) at y=2174000 of the UTM coordinate system; the vertical axis corresponds to the z-coordinate in m.asl.

3.2 Formation modulus

3.2.1. 1-D Elastic Moduli derived from seismic noise and seismicity analysis

One dimensional elastic moduli Es-noise, Es-passive and Ep-passive were calculated for the Los Humeros superhot geothermal system as follows:

- the mean values of 1-D shear wave velocity profile of Los Humeros provided by Dr. Katrin Loeer (HS-Bochum), calculated from ambient seismic noise analysis for the GEMex Deliverable 5.3 on “Seismic structures of the Acoculco and Los Humeros geothermal fields”, chapter 5.7, were used for the calculation of Es-noise;
- the results for the 1D velocity model obtained from analysis of the local seismicity (data collected during the 2018 passive seismic survey carried out by the GEMex consortium), provided by Tania Andrea Toledo Zambrano, GFZ-Potsdam, were used for the calculation of Es-passive and Ep-passive;
- the 3D regional density model of Los Humeros provided by the Mexican partners Marco A. Perez and Dr. Jonathan Carrillo Lopez, CICESE, Earth Sciences Division, calculated by Joint inversion of gravity and magnetic methods assuming a direct relationship between density and magnetization was used in all cases.

The results are presented in Figure 12.

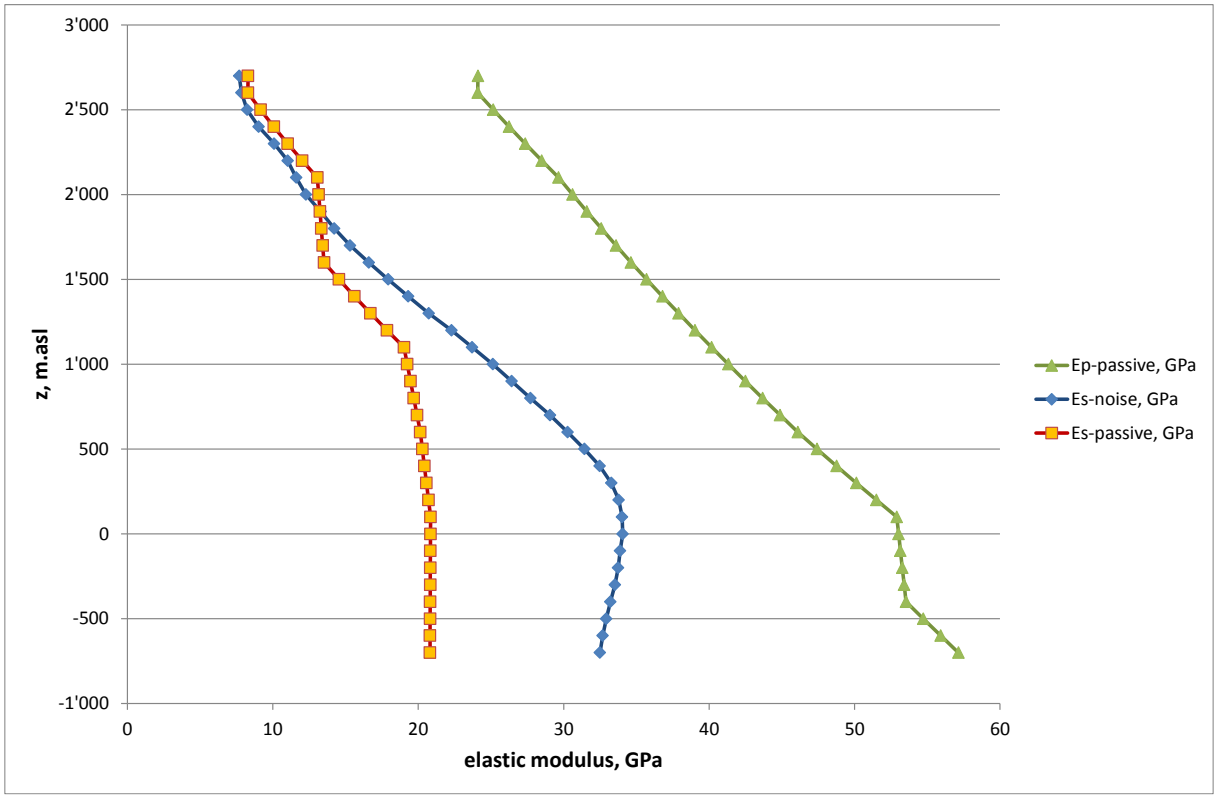

Figure 12: 1-D elastic moduli at Los Humeros superhot geothermal system estimated from a) ambient seismic noise analysis using mean values of Vs, and b) passive seismic analysis using the calculated Vs and Vp at given horizontal layers and interpolating for elevations between them.

The S-wave moduli calculated from ambient noise indicate a steady and almost linear increase with depth down to 250 m asl. At deeper levels the S-wave modulus calculated from ambient noise reduces slightly with depth. Similar trend shows the 1-D S-wave moduli calculated from passive seismic recordings, but it remains approximately stable below 1000 m asl elevation. On the contrary, the 1-D P-wave moduli follow an almost linear trend down to 700 m below sea level.

3.2.2. 3-D Elastic Moduli derived from passive seismic survey

Subsurface 3-D pressure (P-wave modulus, Ep) and shear (S-wave modulus, Es) modulus of elasticity in Los Humeros geothermal field were estimated from passive seismic and gravity models developed by the European and Mexican GEMex partners, as mentioned in chapter 1.2. The resulting elastic moduli (both Ep and Es) at each pair of coordinates in each layer of iso-elevation were estimated using the Kriging interpolation with method = 1.5 (power variogram with exponent equal to 1.5), scaling = 1 and selecting all data points for the interpolation. Their distribution beneath Los Humeros geothermal field is presented in Annex IV and is summarized in Figures 13 to 16 in terms of vertical cross sections.

The cross sections indicate an overall increase of P-wave modulus Ep with depth down to ~2 km below sea level elevation. S-wave modulus Es shows a similar trend, but a maximum values is reached at

certain depth, which remains more or less constant at deeper layers, depending on location. At a given horizontal level (constant elevation) Ep variation is less evident than the variation of Es.

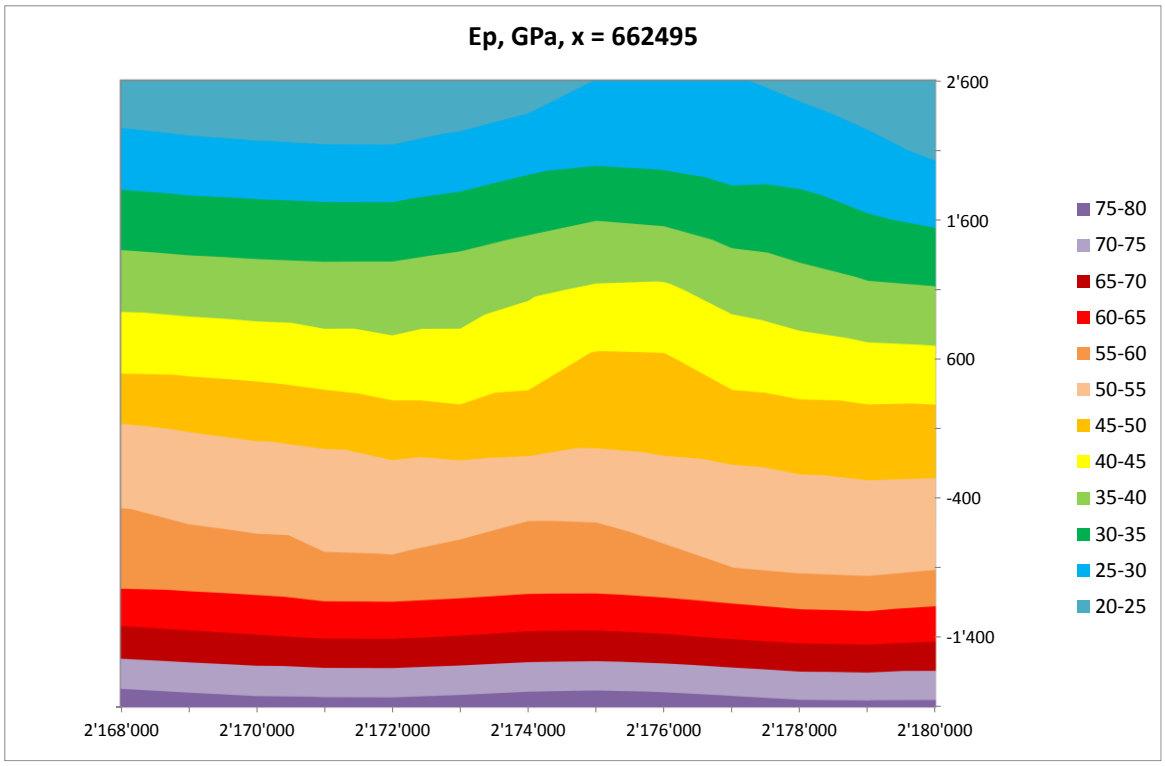

Figure 13: P-wave modulus distribution along a vertical cross section of Los Humeros geothermal field in the direction South (left) – North (right) at x=662495 of the UTM coordinate system; the vertical axis corresponds to the z-coordinate in m.asl

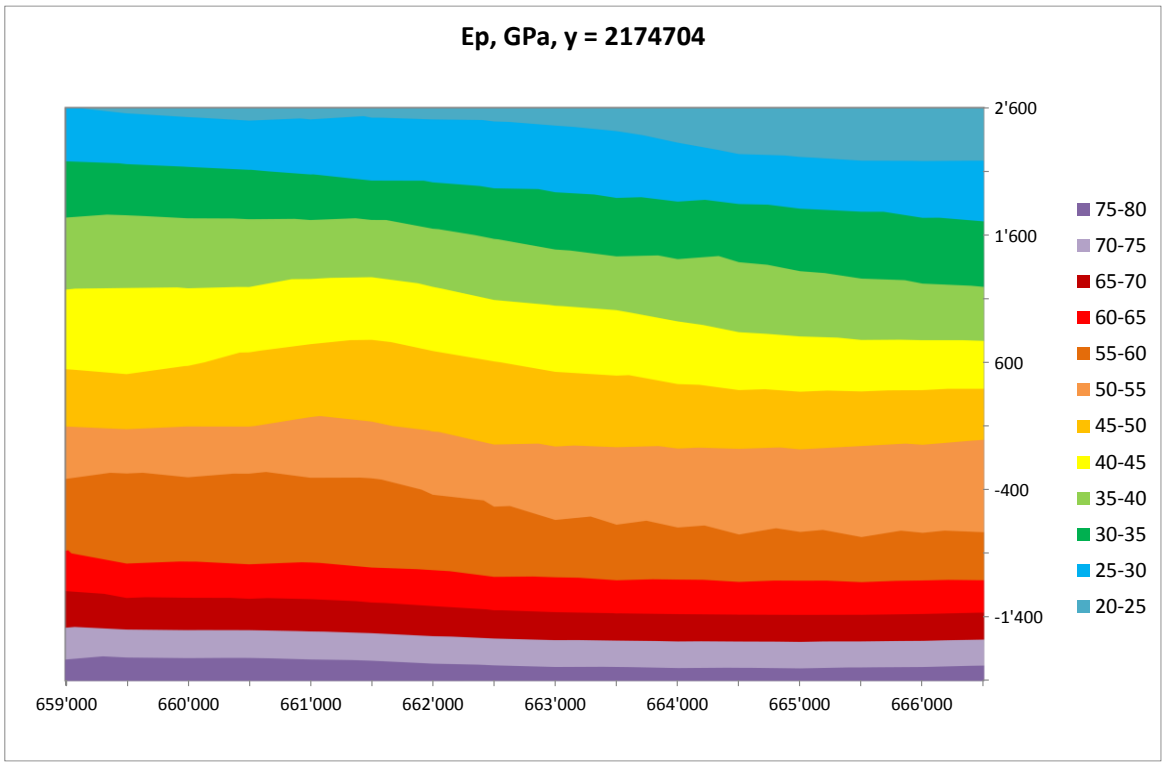

Figure 14: P-wave modulus distribution along a vertical cross section of Los Humeros geothermal field in the direction East (left) -West (right) at y=2174704 of the UTM coordinate system; the vertical axis corresponds to the z-coordinate in m.asl.

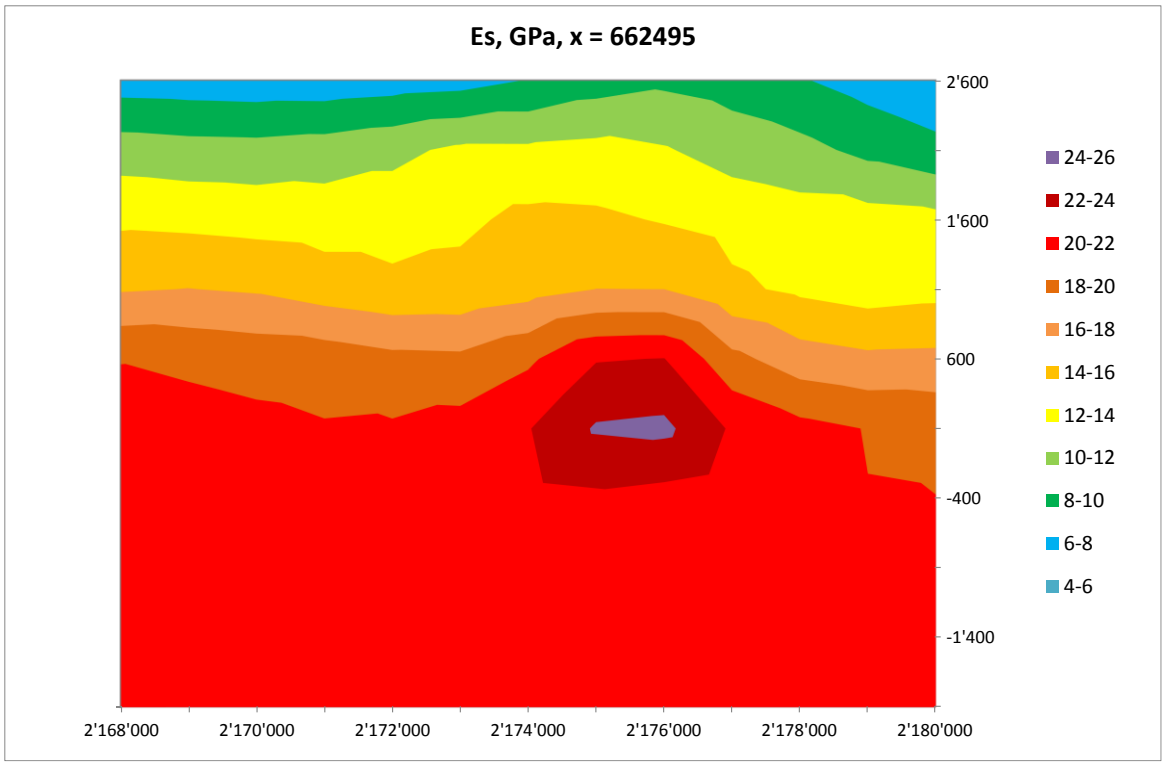

Figure 15: S-wave modulus distribution along a vertical cross section of Los Humeros geothermal field in the direction South (left) – North (right) at x=662495 of the UTM coordinate system; the vertical axis corresponds to the z-coordinate in m.asl

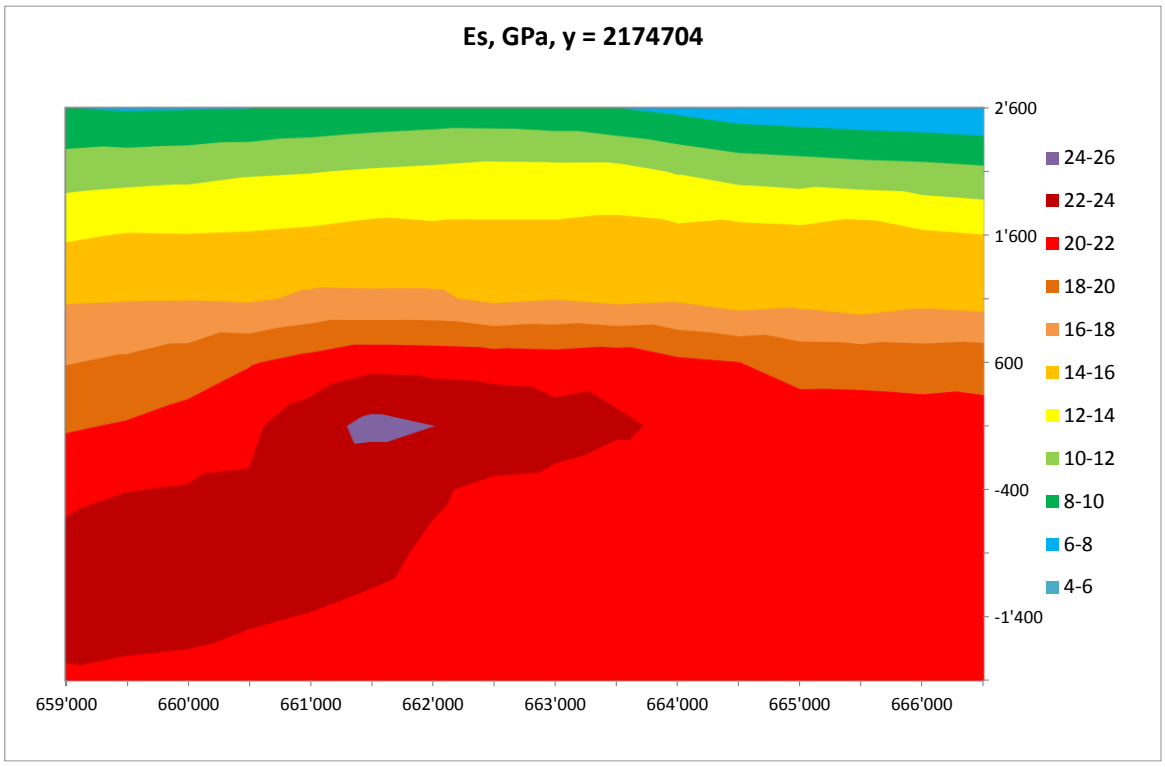

Figure 16: S-wave modulus distribution along a vertical cross section of Los Humeros geothermal field in the direction East (left) -West (right) at y=2174704 of the UTM coordinate system; the vertical axis corresponds to the z-coordinate in m.asl.

3.2.3. Elastic Moduli derived from active seismic survey

The P-wave seismic velocities at well locations in Los Humeros geothermal field were calculated by OGS by migration velocity analysis (common image gathers) inverting the processed data, using the legacy data provided by CFE, which were recorded during the active seismic survey carried out at Los Humeros in 1998 (see D5.3). 37 wells were selected for the calculations, which correspond to the ones located on, nearby, or between the four seismic lines (see Figure 8). The results are presented in detail in Annex V and are summarized in Figure 17, which presents the relationship of Vp with depth in terms of elevation above sea level.

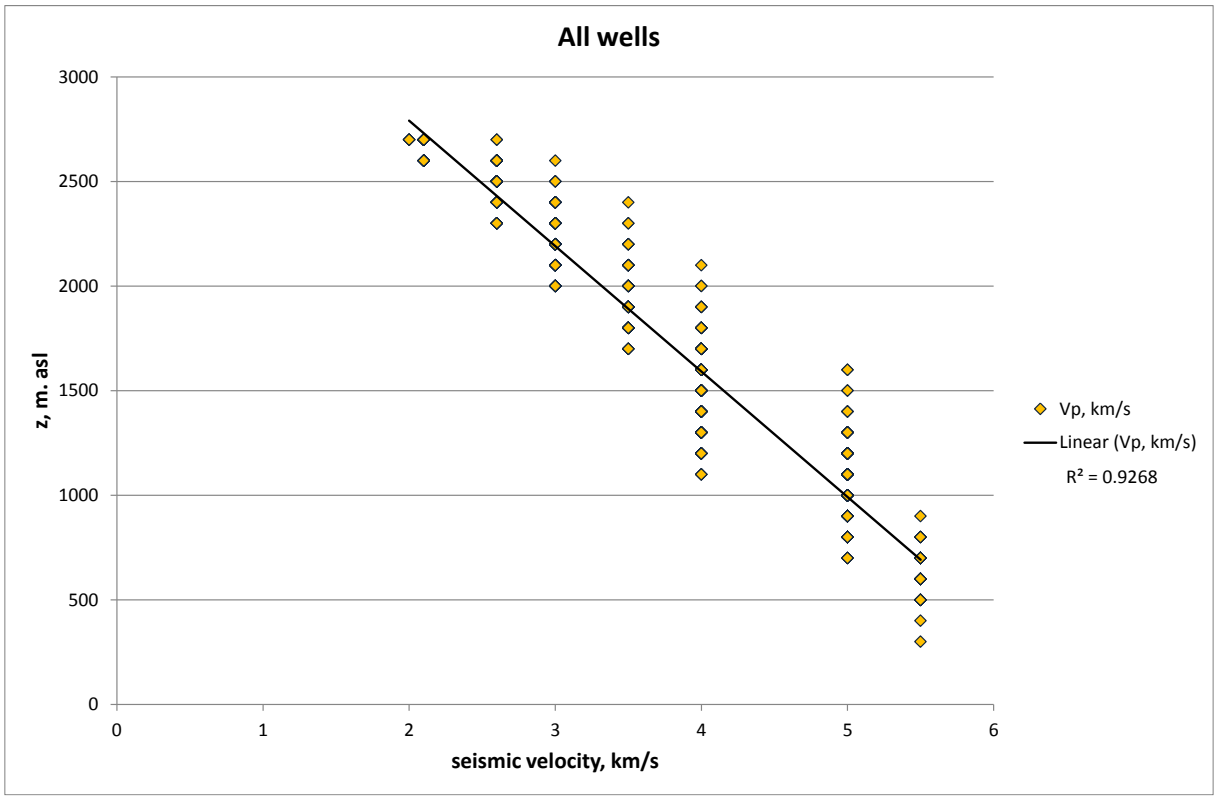

Figure 17: P-wave velocity as derived by inversion of the 1998 active seismic survey data in 37 deep wells in Los Humeros

Using the regional density model of Los Humeros, the P-wave elastic moduli were also calculated for each one of the 37 wells mentioned above, which are presented in detail in Annex V and are summarized in Figure 18.

The clusters of points appearing in both Figures are attributed to the different layers of equal Vp used in the inversion. The points are more scattered in the Es vs z graph, due to the variation of density, as the regional density model provides a 3-D continuous density array.

Figure 17 indicates a weak linear relationship between P-wave velocity with elevation with $R^2 = 92.68\%$. A regression analysis was also done to check possible relationship of seismic velocity Vp with in situ rock density, which indicated no statistically significant relationship ($R^2 = 12\%$), as shown in Figure 19.

The relation of P-wave modulus with elevation is presented in Figure 18, where due to the spread of the data points, it is possible to fit both a second order polynomial and a linear curve. The corresponding R^2 values are 91.03% for the 2nd order polynomial and 89.32% for the linear curve fit.

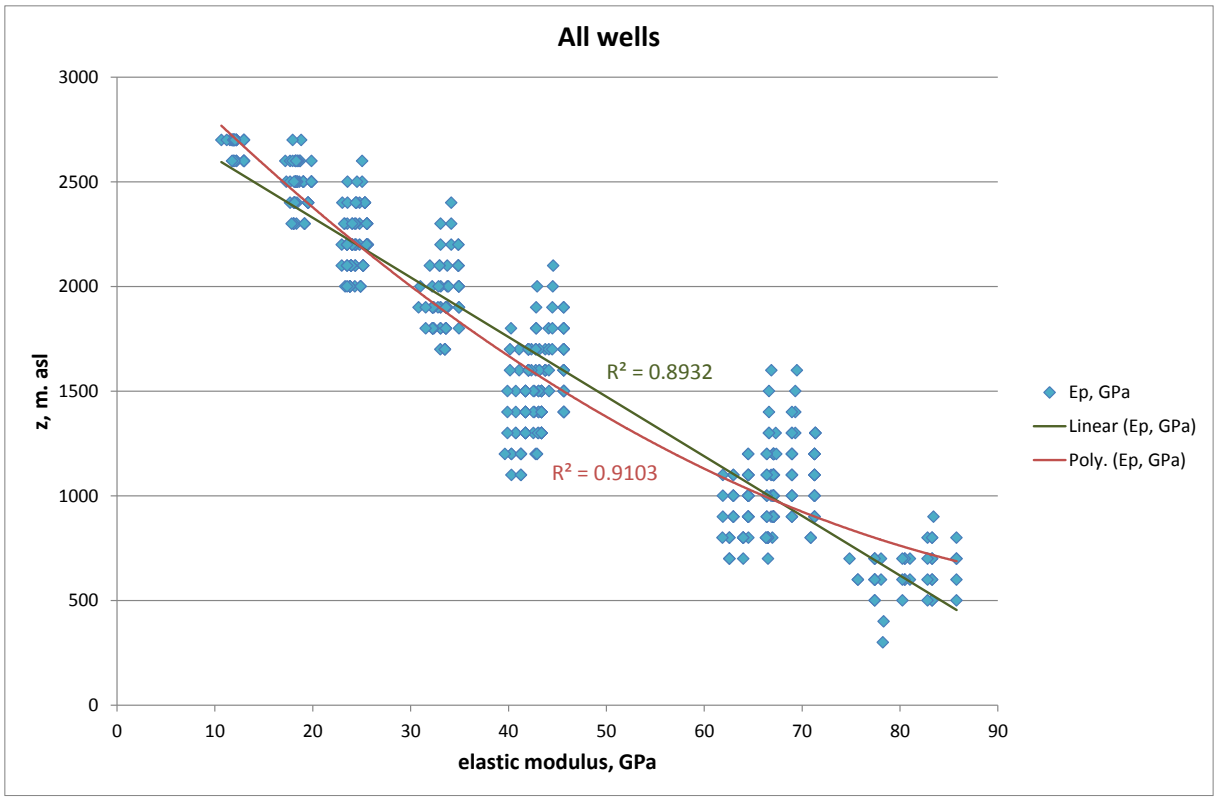

Figure 18: P-wave modulus as derived by inversion of the legacy 1998 active seismic survey data in 37 deep wells in Los Humeros

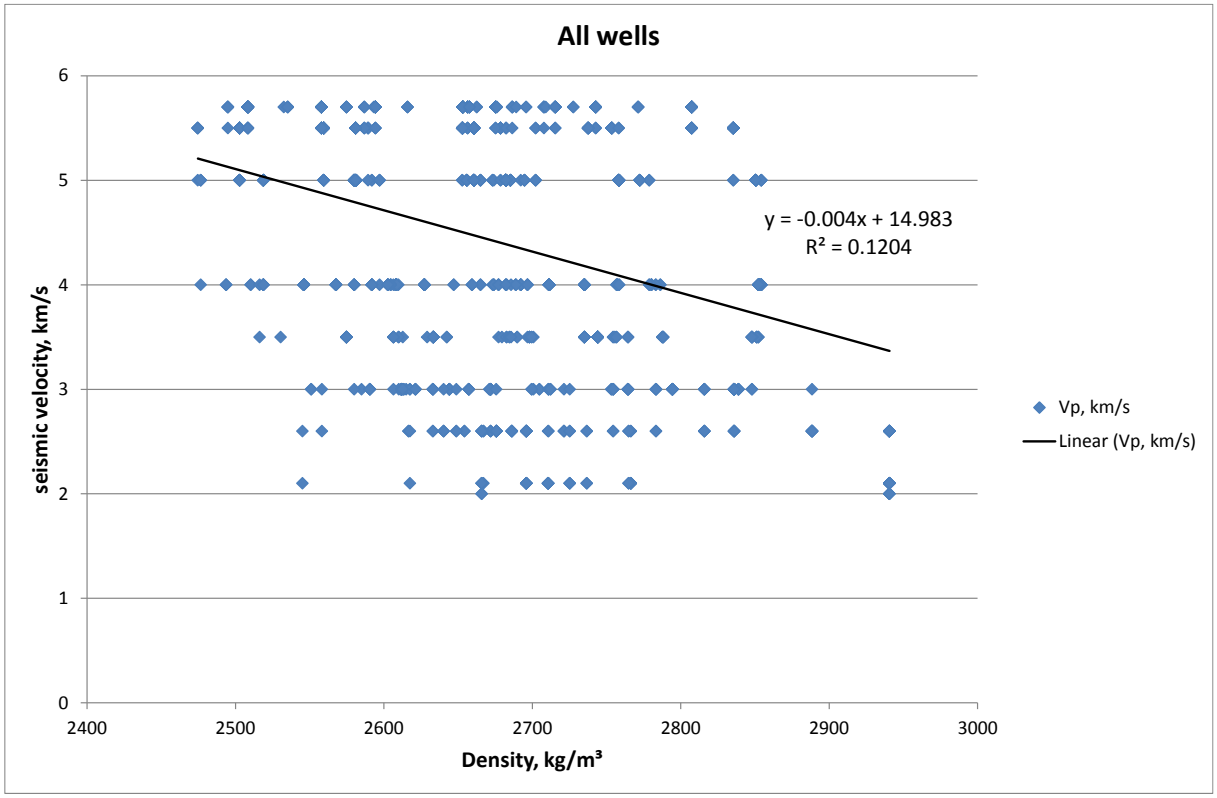

Figure 19: Plot of P-wave velocity versus density, indicating no correlation between the two parameters.

3.3 Correlation to temperature

3.3.1 Ambient seismic noise analysis

The correlation of S-wave ambient seismic noise velocity (average values) with temperature is presented in Figure 20, together with the S-wave and P-wave velocities calculated from inversion of passive seismic data. The graphs indicate statistically significant exponential relationships with R^2 higher than 95% for the S-wave velocities and higher than 90% for the P-wave velocities. If a second order polynomial interpolation is considered higher than 95% R^2 values are obtained.

Similar results are derived when correlating S-wave ambient seismic noise moduli with temperature, as shown in Figure21, where P-wave and S-wave elastic moduli derived from passive seismic survey are also presented.

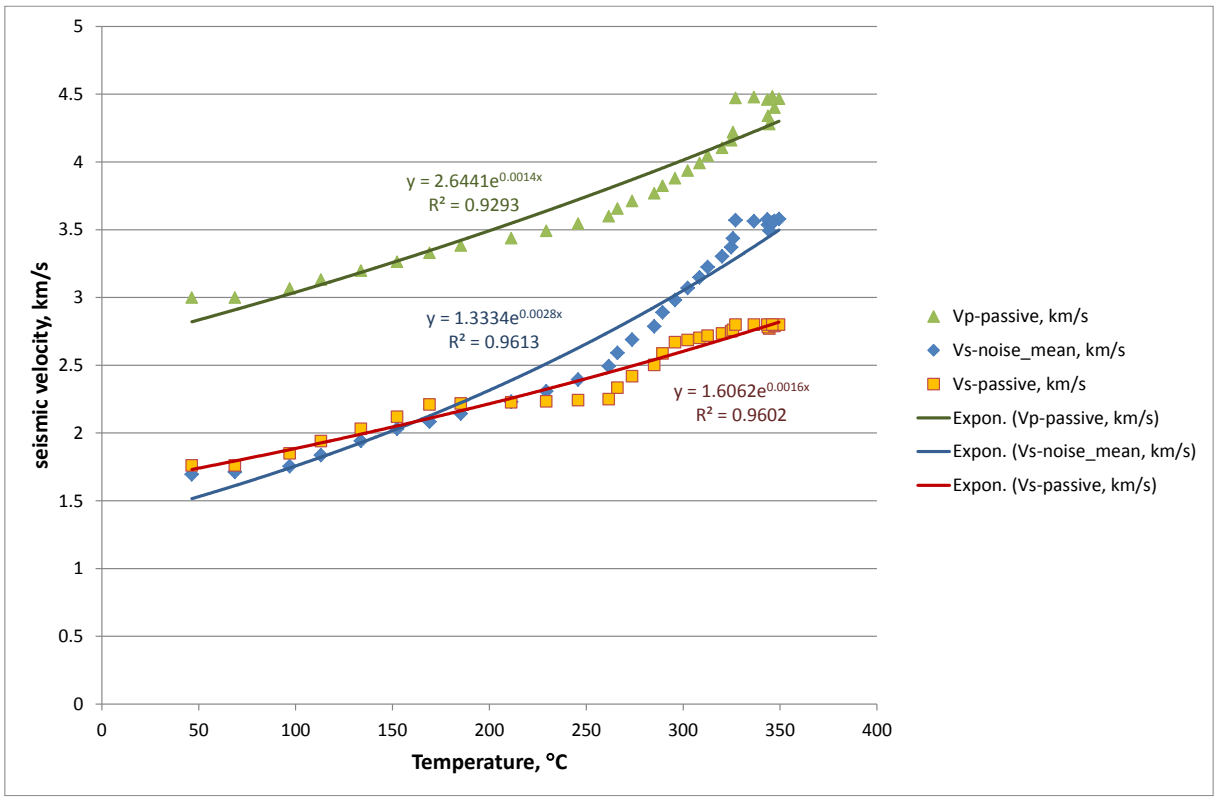

Figure 20: P-wave and S-wave velocities as derived by ambient noise and 1-D passive seismic surveys as a function of temperature and best fit exponential trendlines.

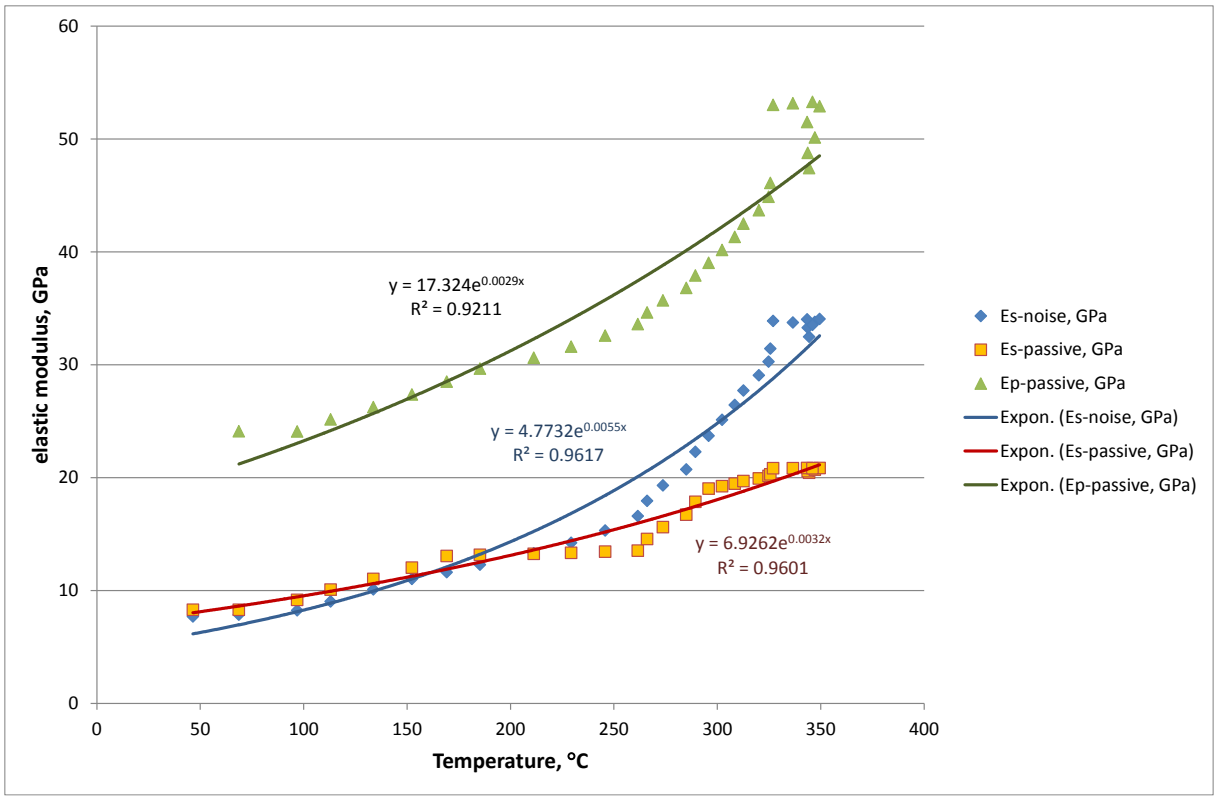

Figure 21: P-wave and S-wave modulus as derived by ambient noise and passive seismic surveys as a function of temperature and best fit exponential trendlines.

3.3.2 Passive seismic survey

A detailed three dimensional statistical analysis and correlations of P-wave and S-wave velocities derived from the inversion of recorded seismicity during 2017-2018 in Los Humeros is presented in Annexes 6-12 as follows.

- Overall models examining the relation between T and Vp, Ep, Vs and Es are presented in Annex 10. Overall models examining the relation between T and the centred and normalized values of Vp, Ep, Vs and Es are presented in Annex 12.
- Overall models examining the relation between Z and Vp, Ep, Vs and Es are presented in Annex 11.
- Individual models per well and individual model per elevation level (Z) examining the relation of T with Vp and Vs are presented in Annexes 6 and 8 respectively.
- Individual models per well and individual model per elevation level (Z) examining the relation of T with Ep and Es are presented in Annexes 7 and Annex 9 respectively.

A summary of results is shown in Figures 22 (seismic velocities) and 23 (elastic moduli), where matching pairs of these seismic and elastic parameters with temperature from all Los Humeros wells are depicted.

The results indicate statistically significant but weak correlation of seismic velocities and elastic moduli with temperature, as the corresponding R^2 is slightly above 70%, when an exponential best fit is considered. A second order polynomial interpolation, yields similar results.

All wells

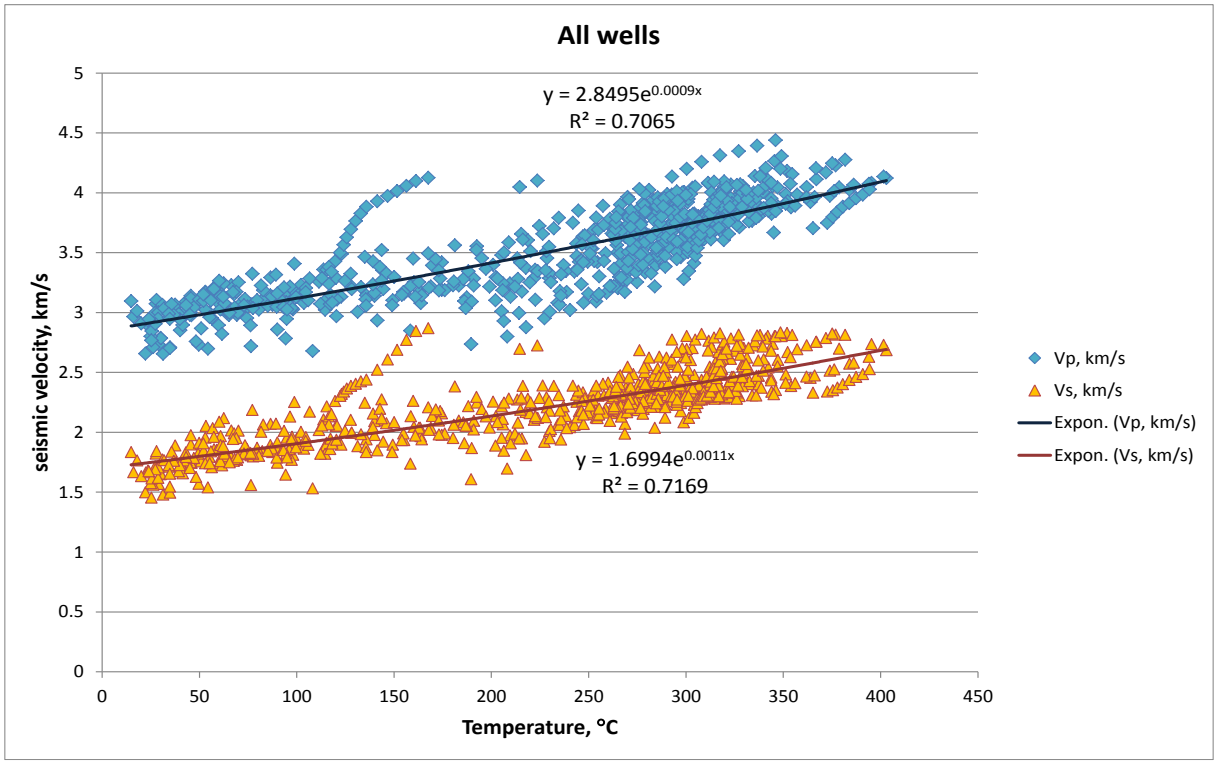

Figure 22: P-wave and S-wave velocities as derived by 3-D passive seismic survey as a function of temperature indicating a weak relation with R^2 just above 70%.

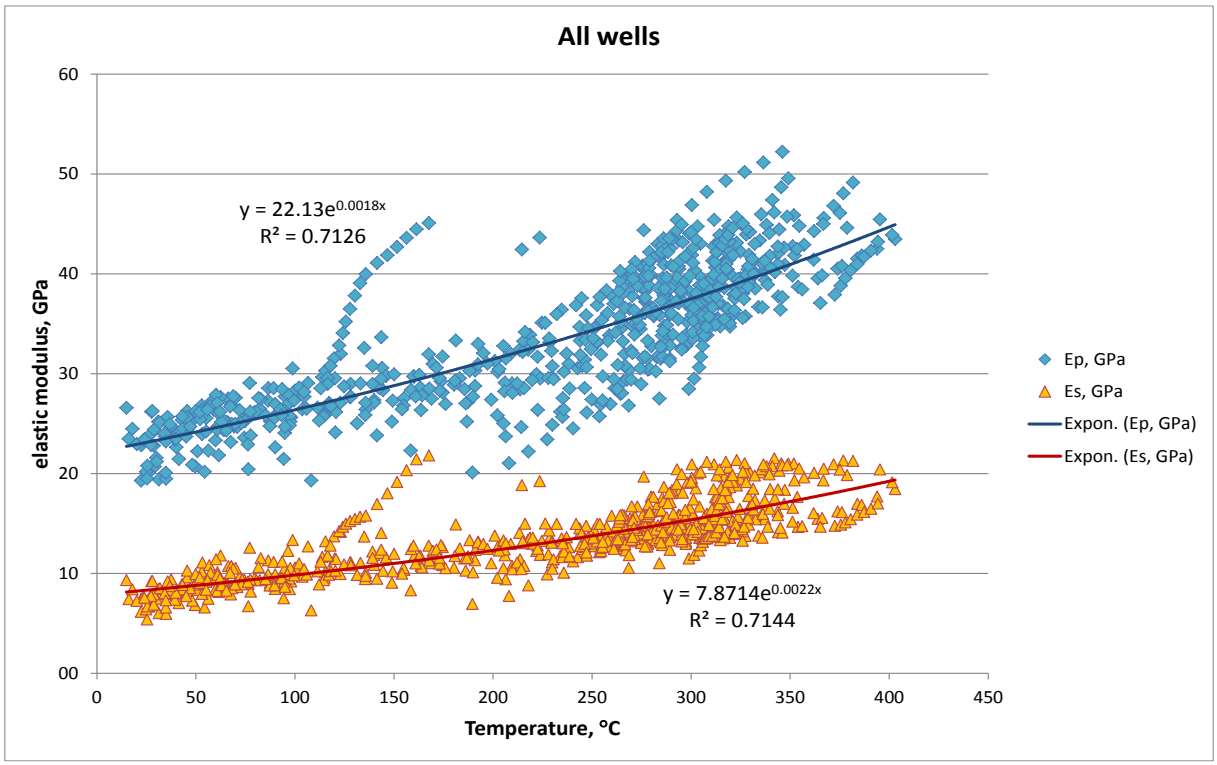

Figure 23: P-wave and S-wave modulus as derived by 3-D passive seismic survey as a function of temperature indicating a weak relation with R^2 just above 70%.

Regional vs local gravity models

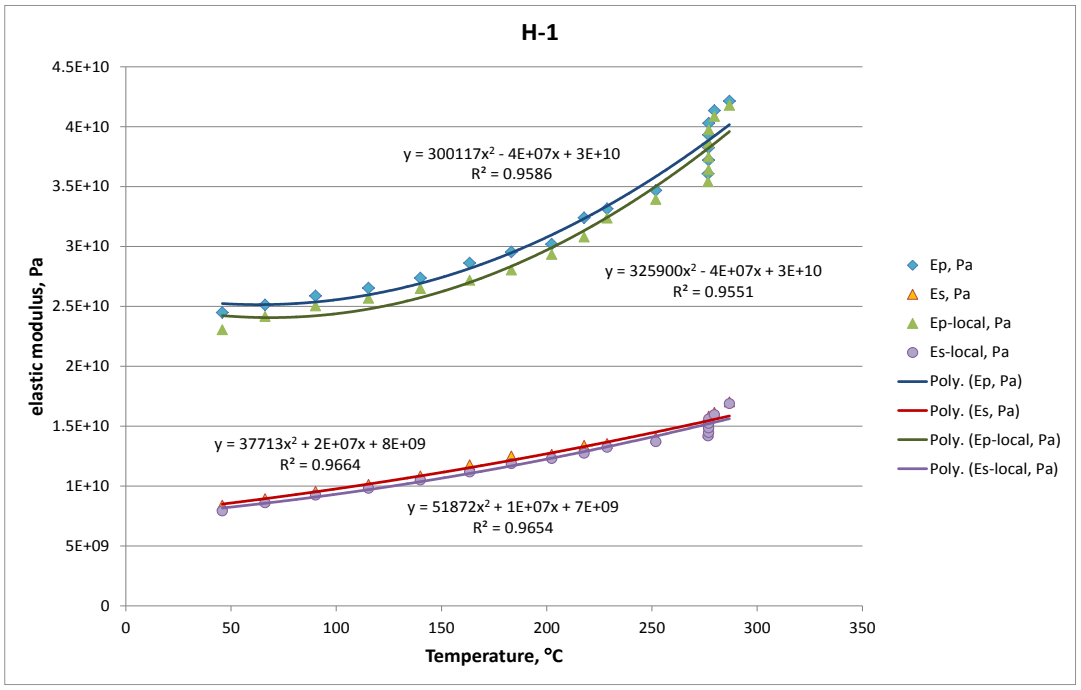

Figure 24: P-wave and S-wave moduli as a function of temperature in well H-1 using densities from regional and local gravity models: resulting differences are minor.

Figure 24 illustrates a comparison of results when using local density model instead of the regional density one, indicating that resulting differences are minor. Figure 24 also illustrates, that for a given well location statistically strong correlations can be derived between Elastic moduli and temperature, a pattern that is followed in all geothermal wells in Los Humeros. However, the correlating function parameters differ from well to well, resulting in a weak overall correlation when all data points are considered, as shown in Figures 22 and 23.

Horizontal layers

The analysis presented until now, indicates that there is a statistically significant relationship between rock moduli and temperature in the vertical direction, expressed by exponential and second order polynomial functions. This relationship is strong in case of one dimensional analysis, as well as in the case of individual deep wells, but it is weak when three dimensional results are considered.

In order to eliminate the effect of the vertical direction, elastic moduli are plotted against temperature in horizontal slices, each one of which corresponds to a constant elevation above sea level. The results are presented in Annexes 8 and 9 and are summarised in Figures 25 to 30, which show that there is no statistically significant correlation between elastic moduli and temperature at the same elevation level z, as the corresponding R^2 values are very low, in the range 0-21%.

In general, small variations of elastic moduli are observed within a horizontal layer, while there are large variations of temperature. The temperature variations are a result of the fluid flow patterns, which depend on the subsurface structural layout, as the main fault zones (see Figure 8) provide the pathways for the upflow of deeper superhot fluids.

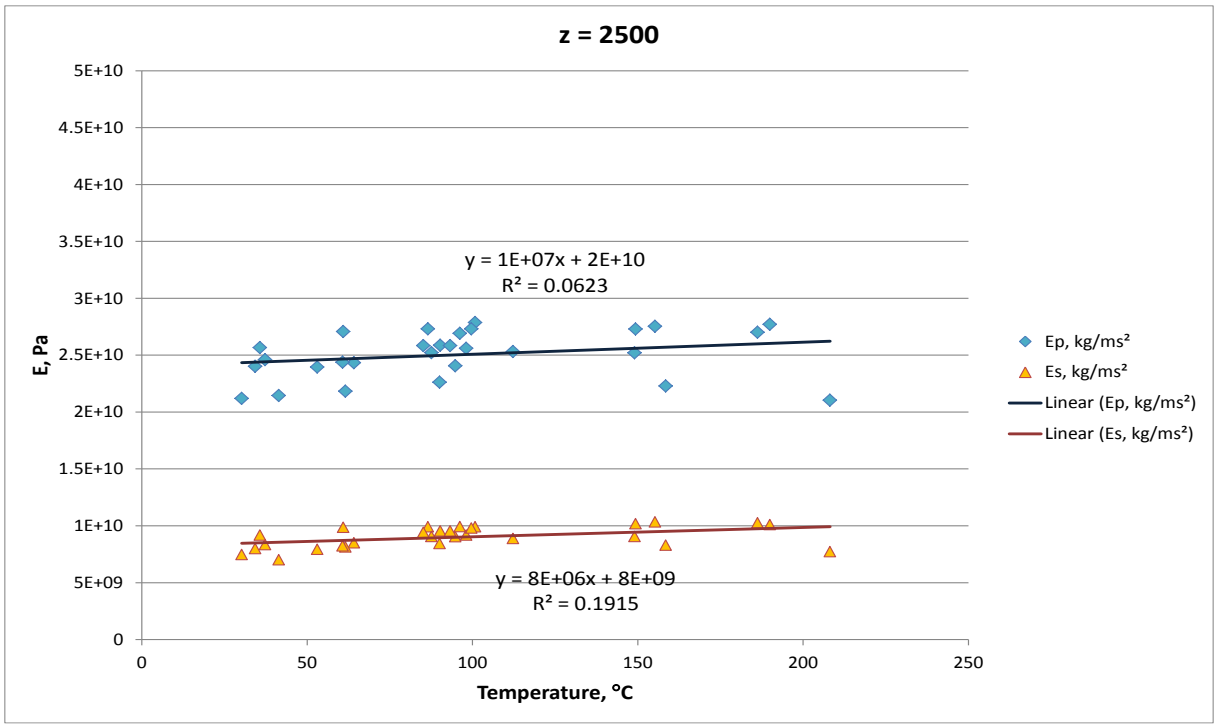

Figure 25: P-wave and S-wave moduli as derived by 3-D passive seismic survey and regional density model as a function of temperature at the same horizontal surface (z=2500 m asl), indicating no statistically significant relationship between the two parameters.

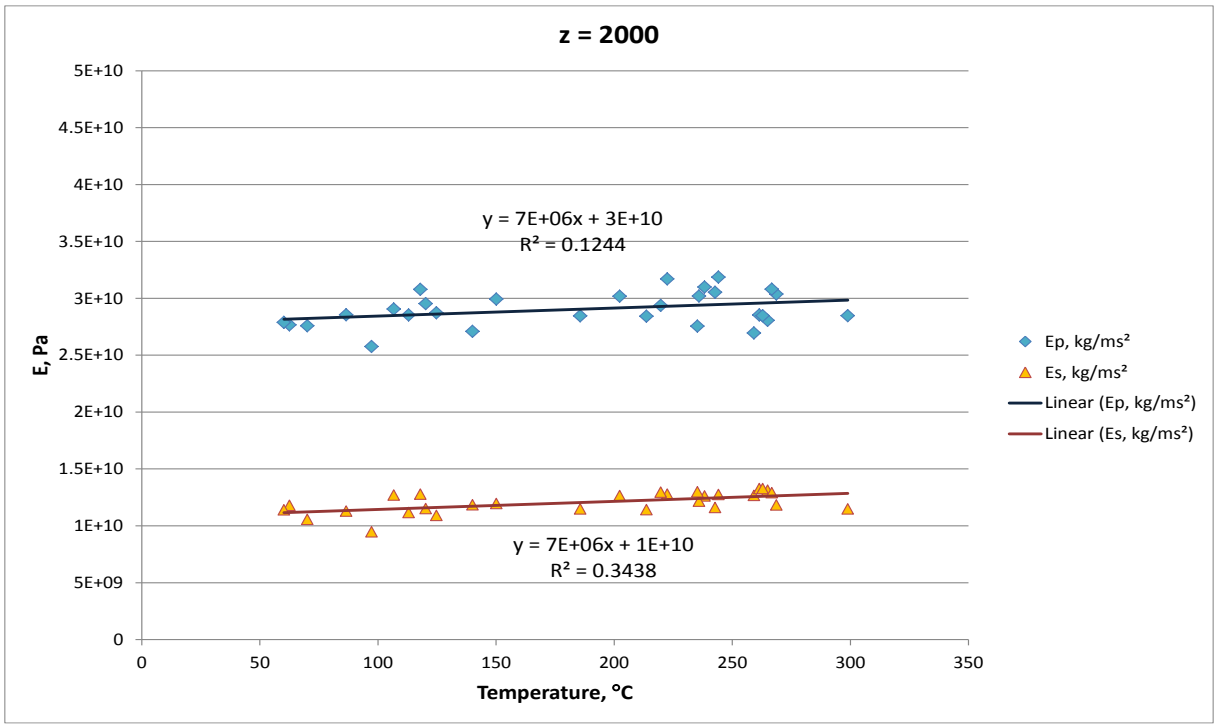

Figure 26: P-wave and S-wave moduli as derived by 3-D passive seismic survey and regional density model as a function of temperature at the same horizontal surface (z=2000 m asl), indicating no statistically significant relationship between the two parameters.

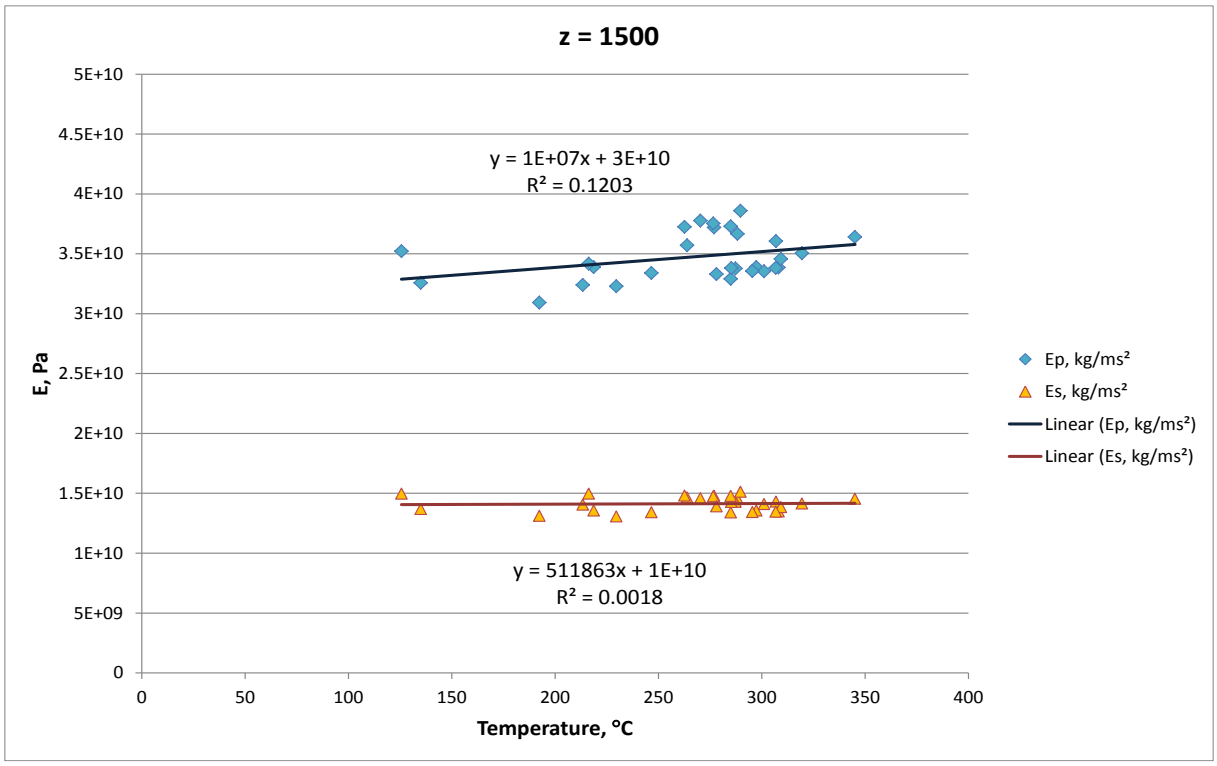

Figure 27: P-wave and S-wave moduli as derived by 3-D passive seismic survey and regional density model as a function of temperature at the same horizontal surface (z=1500 m asl), indicating no statistically significant relationship between the two parameters.

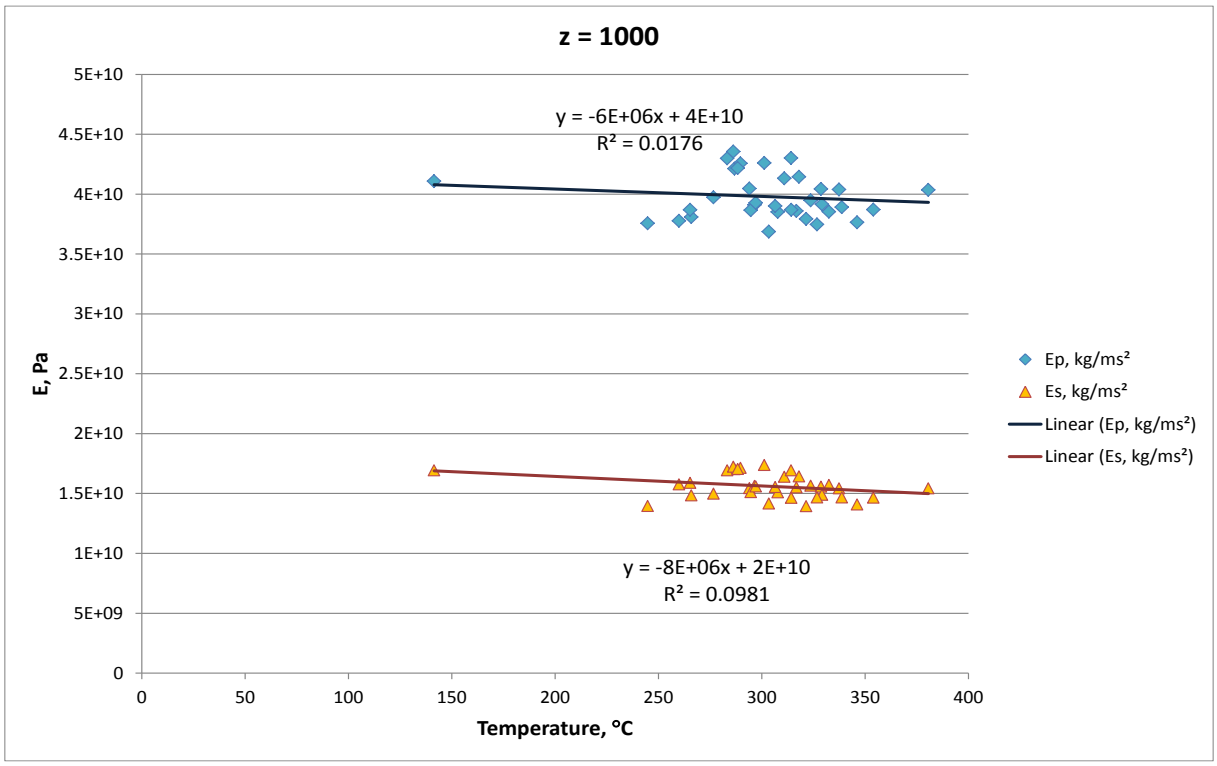

Figure 28: P-wave and S-wave moduli as derived by 3-D passive seismic survey and regional density model as a function of temperature at the same horizontal surface (z=2000 m asl), indicating no statistically significant relationship between the two parameters.

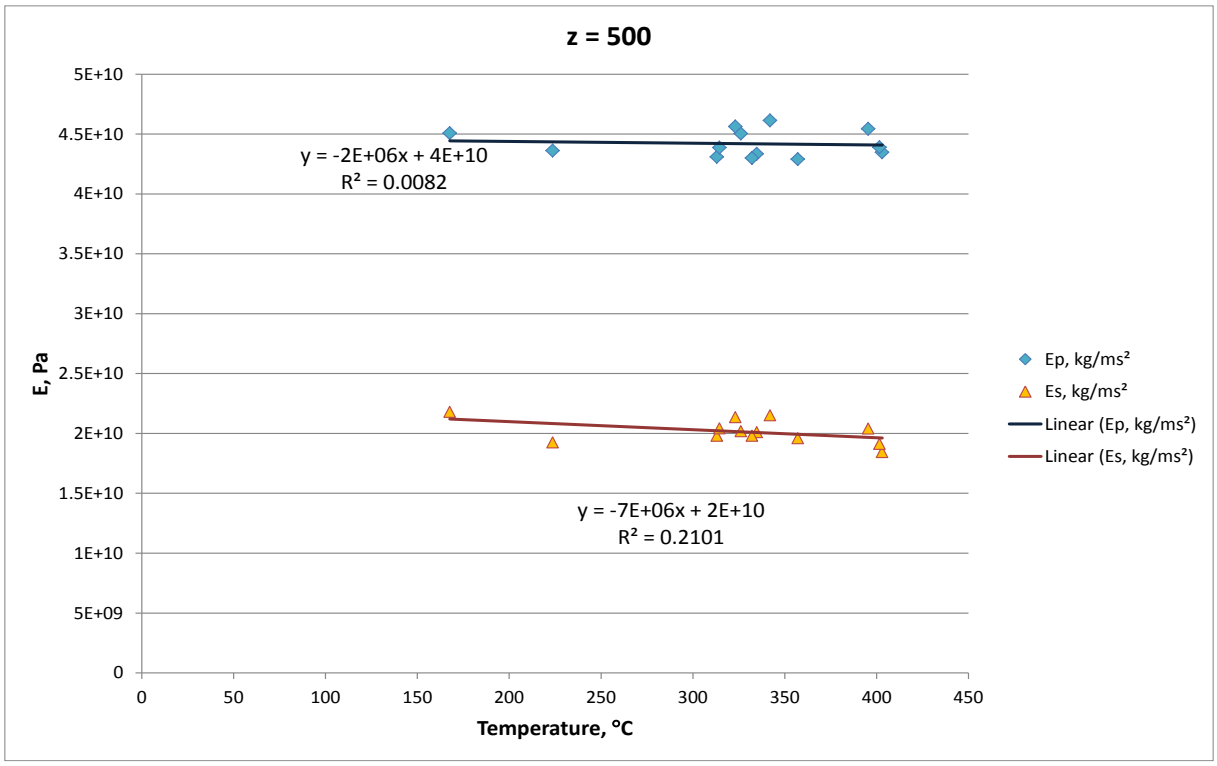

Figure 29: P-wave and S-wave moduli as derived by 3-D passive seismic survey and regional density model as a function of temperature at the same horizontal surface (z=500 m asl), indicating no statistically significant relationship between the two parameters.

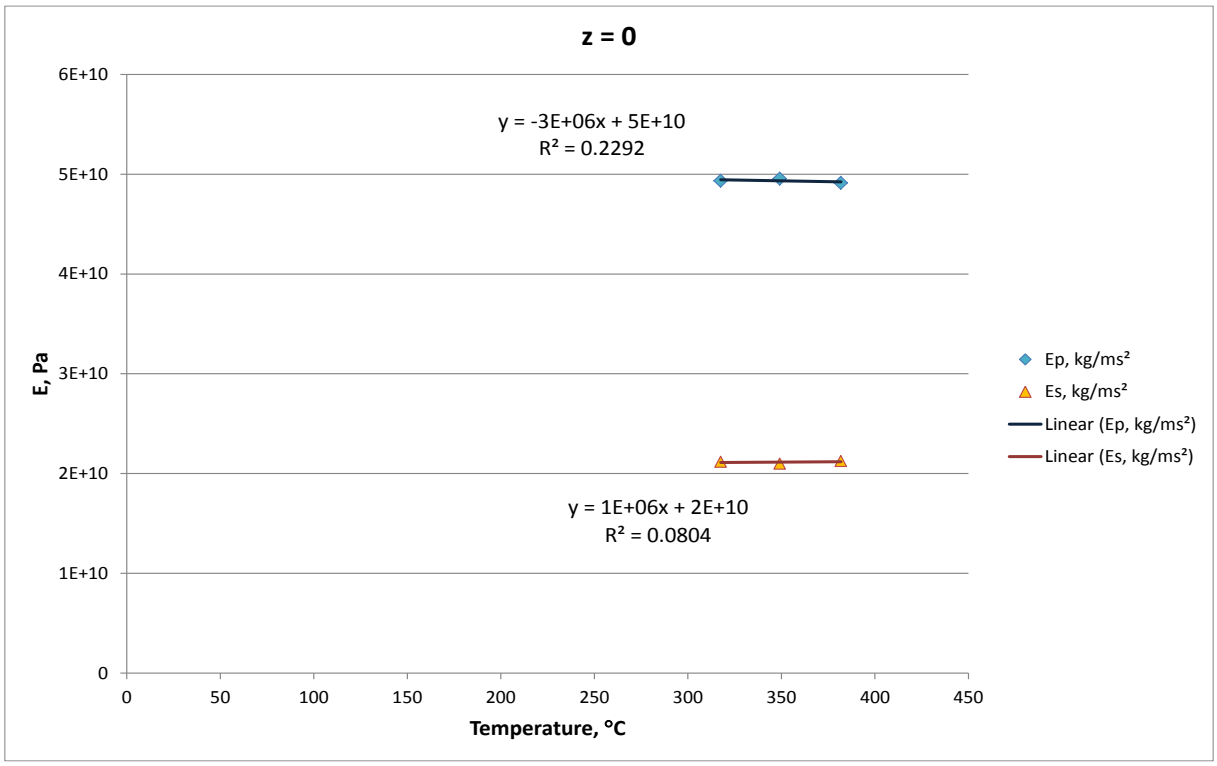

Figure 30: P-wave and S-wave moduli as derived by 3-D passive seismic survey and regional density model as a function of temperature at the same horizontal surface (z=0 m asl), indicating no statistically significant relationship between the two parameters.

In order to provide an integrated statistical evaluation of all data, the average (mean) values of seismic velocities $\overline{V}$ p and $\overline{V}$ s and elastic moduli $\overline{E}$ p and $\overline{E}$ s are calculated at each level of elevation. Then, the statistical analysis is performed by introducing centred and normalized variables as shown in Table 3.1, where SD is the standard deviation:

Variable	Mean value at same elevation	Centred variable	Normalized variable
Vp	$\overline{V}$ p	Vp – $\overline{V}$ p	(Vp – $\overline{V}$ p) / SD
Vs	$\overline{V}$ s	Vs – $\overline{V}$ s	(Vs – $\overline{V}$ s) / SD
Ep	$\overline{E}$ p	Ep – $\overline{E}$ p	(Ep – $\overline{E}$ p) / SD
Es	$\overline{E}$ s	Es – $\overline{E}$ s	(Es – $\overline{E}$ s) / SD

Table 3.1: Centred and normalized variables

The analysis is presented in Annex 12 and indicates no statistical significant correlation of above variables with temperature, as R^2 is less than 7.5% in all cases.

3.3.3 Active seismic survey

A detailed analysis and correlations of P-wave velocities derived from the processing performed by OGS with depth migration velocity analysis (Common Image Gathers, CIG) and inversion of active seismic data of 1998 in Los Humeros (see GEMex D5.3) interpolated and extrapolated at the well locations, is presented in Annexes 5-12, as follows.

- Visualization of available data points in each one of the 37 Los Humeros wells located between the seismic lines and best fit exponential correlation of Vp and Ep with temperature are presented in Annex 5.
- Overall models examining the relation between T and Vp, Ep are presented in Annex 10. Overall models examining the relation between T and the centred and normalized values of Vp, Ep are presented in Annex 12.
- Overall models examining the relation between Z and Vp, Ep are presented in Annex 11.
- Individual models per well and individual model per elevation level (Z) examining the relation of T with Vp are presented in Annexes 6 and 8 respectively.
- Individual models per well and individual model per elevation level (Z) examining the relation of T with Ep are presented in Annexes 7 and Annex 9 respectively.

In this analysis the seismic velocity results and model obtained by the first-stage inversion were utilized. This result is based on horizon interpretation (D5.3) and is in current phase of revision by data integration in the framework of the GEMex project Task 5.4. In this sense the following results have to be considered as preliminary results by active seismic data of Los Humeros in the local model (restricted area with respect to the regional one used for passive data), and further improvements will be investigated in subsequent phases of the data integration.

A summary of results is shown in Figures 31 (P-wave velocities) and 32 (P-wave moduli), where matching pairs of these seismic and elastic parameters with temperature from all Los Humeros wells are depicted.

The results indicate statistically significant but weak correlation of seismic velocities and elastic moduli with temperature, as the corresponding R^2 is slightly less than 70%, when an exponential best fit is considered. A second order polynomial interpolation yields similar but less significant results with R^2 values in the range 61-66%.

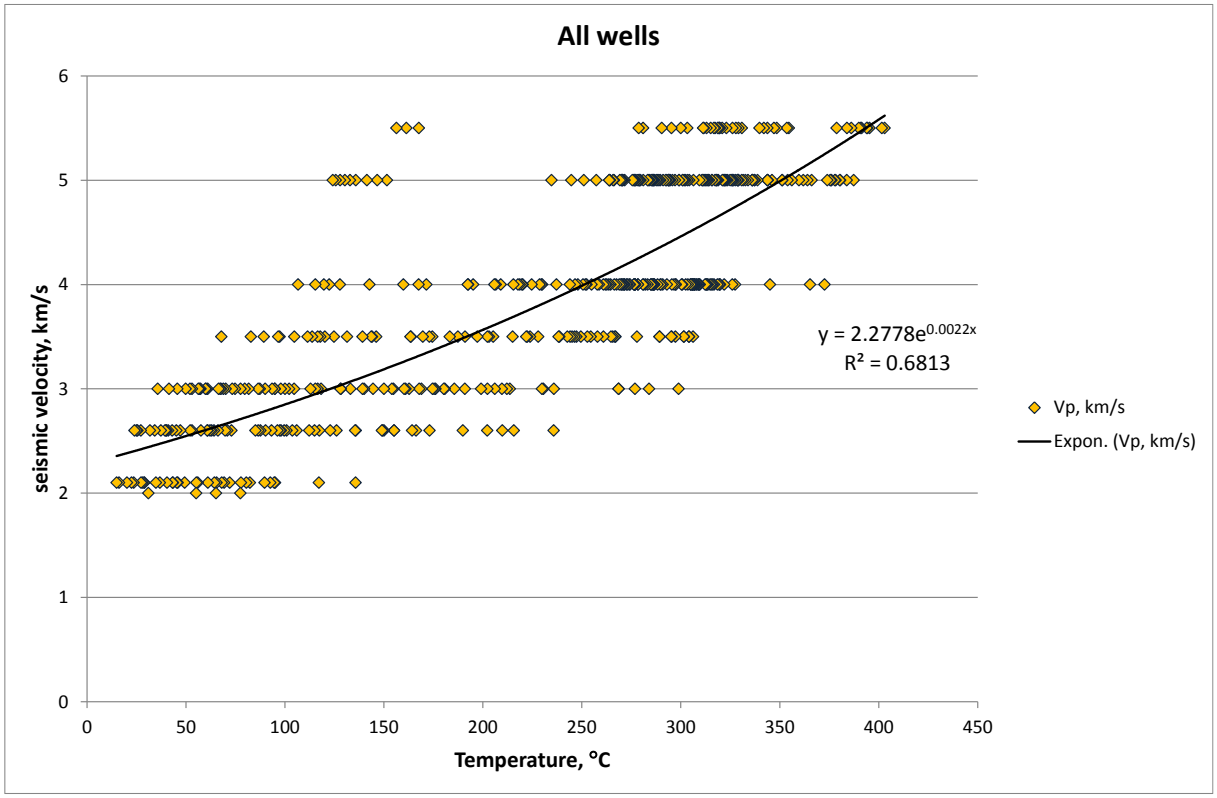

Figure 31: P-wave velocity as derived by 1998 active seismic survey as a function of temperature indicating a weak relation with R^2 just below 70%.

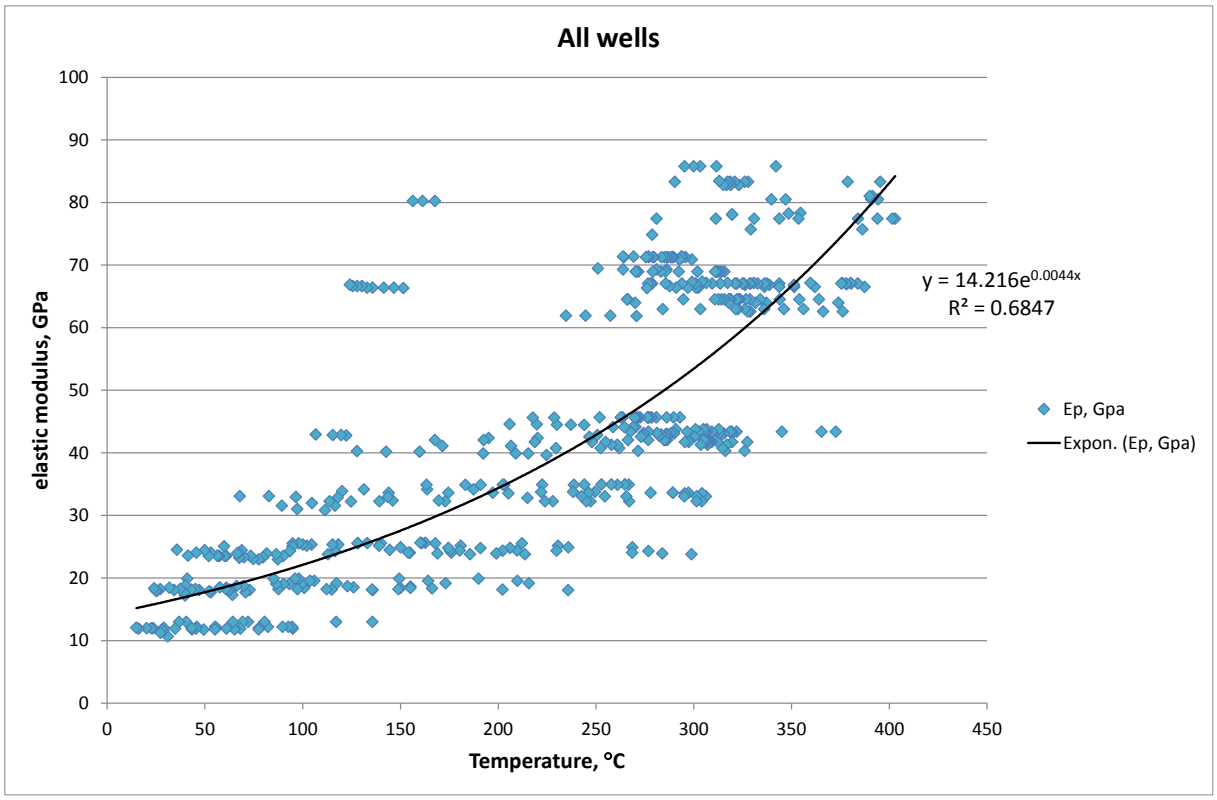

Figure 32: P-wave elastic modulus as derived by 1998 active seismic survey as a function of temperature indicating a weak relation with R^2 just below 70%.

The same analysis has been carried out for each one of the 37 deep wells located between the four seismic lines of Figure 8, which proved that in each well an exponential best fit of the P-wave velocity – temperature and elastic modulus – temperature pairs is possible with the corresponding R^2 values lying in the range 73-100%. The same conclusion as in the case of passive seismic surveys is reached, namely that there is a weak or strong statistically significant relationship between P-wave velocities and elastic moduli with temperature in the vertical direction.

Horizontal layers

In order to eliminate the z-direction effect a set of horizontal slices are considered, each one corresponding to a single elevation values, where correlations between P-wave velocities and moduli with temperature are derived by regression analysis. The results are presented in Annexes 8 and 9 and are summarised in Figures 33-37 for P-wave velocities and in Figures 38-42 for P-wave moduli. In all cases no statistical significant relationship is evident, as the corresponding R^2 values are below 28% in all cases.

Integrated statistical analysis is also performed by introducing centred and normalized variables according to Table 3.1. The analysis is presented in Annex 12 and indicates no statistical significant correlation of above variables with temperature, as R^2 is less than 1% in all cases. It must be noted however, that in this case we utilized 3D data laterally extrapolated and interpolated to fit the well positions starting from the four seismic lines with crossing geometries (see GEMex D5.3).

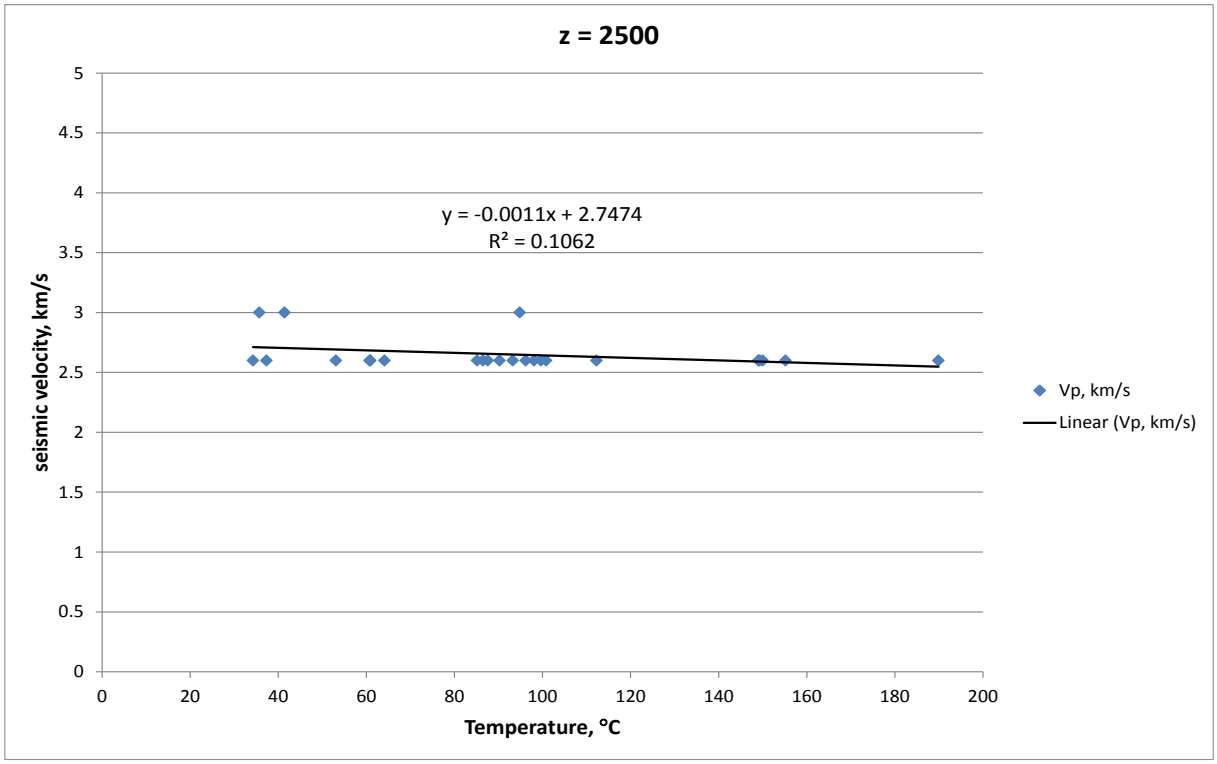

Figure 33: P-wave velocity as derived by the 1998 active seismic survey as a function of temperature at the same horizontal surface (z=2500 m asl), indicating no statistically significant relationship between the two parameters.

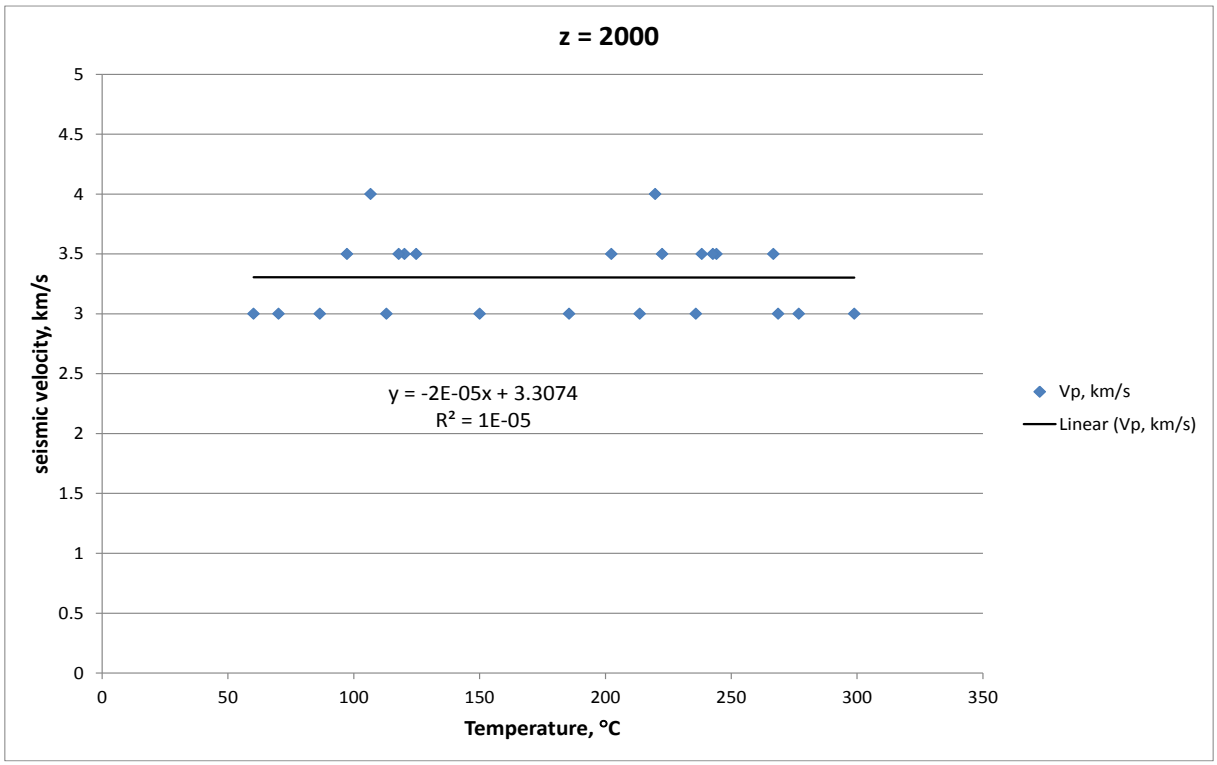

Figure 34: P-wave velocity as derived by the 1998 active seismic survey as a function of temperature at the same horizontal surface (z=2000 m asl), indicating no statistically significant relationship between the two parameters.

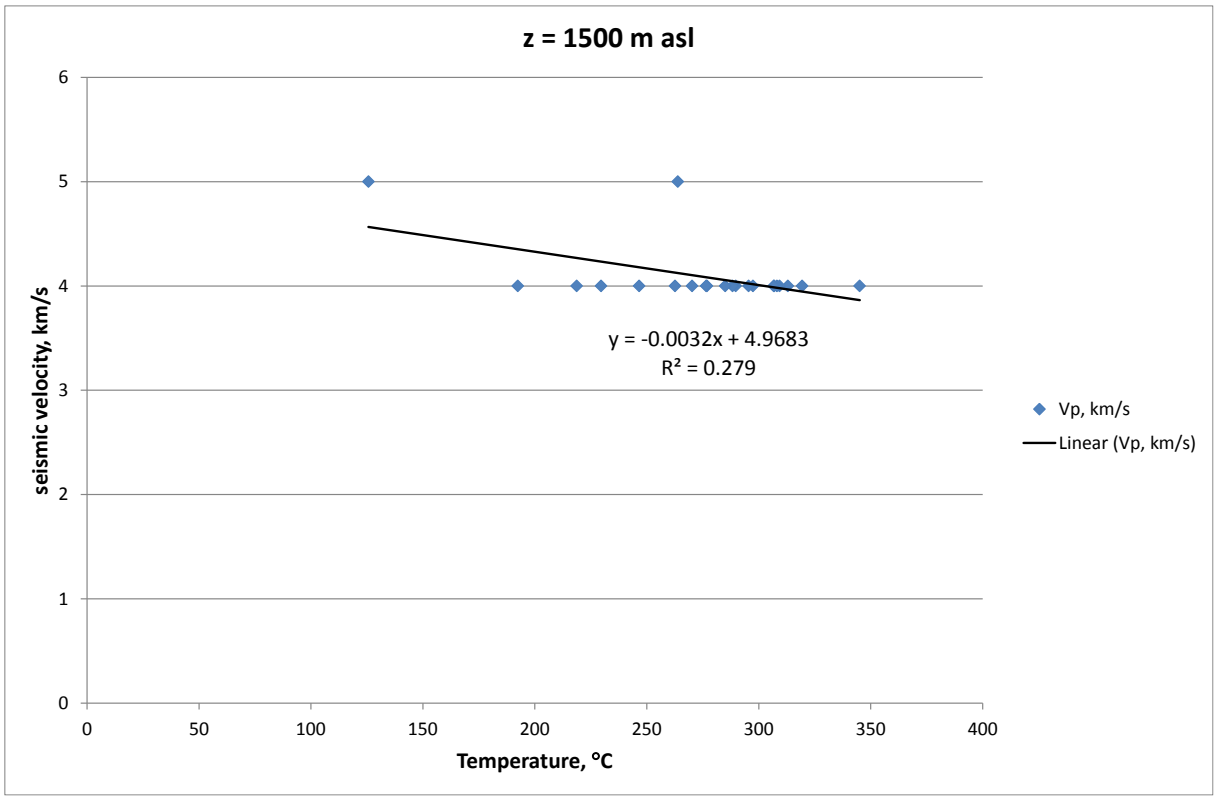

Figure 35: P-wave velocity as derived by the 1998 active seismic survey as a function of temperature at the same horizontal surface (z=1500 m asl), indicating no statistically significant relationship between the two parameters.

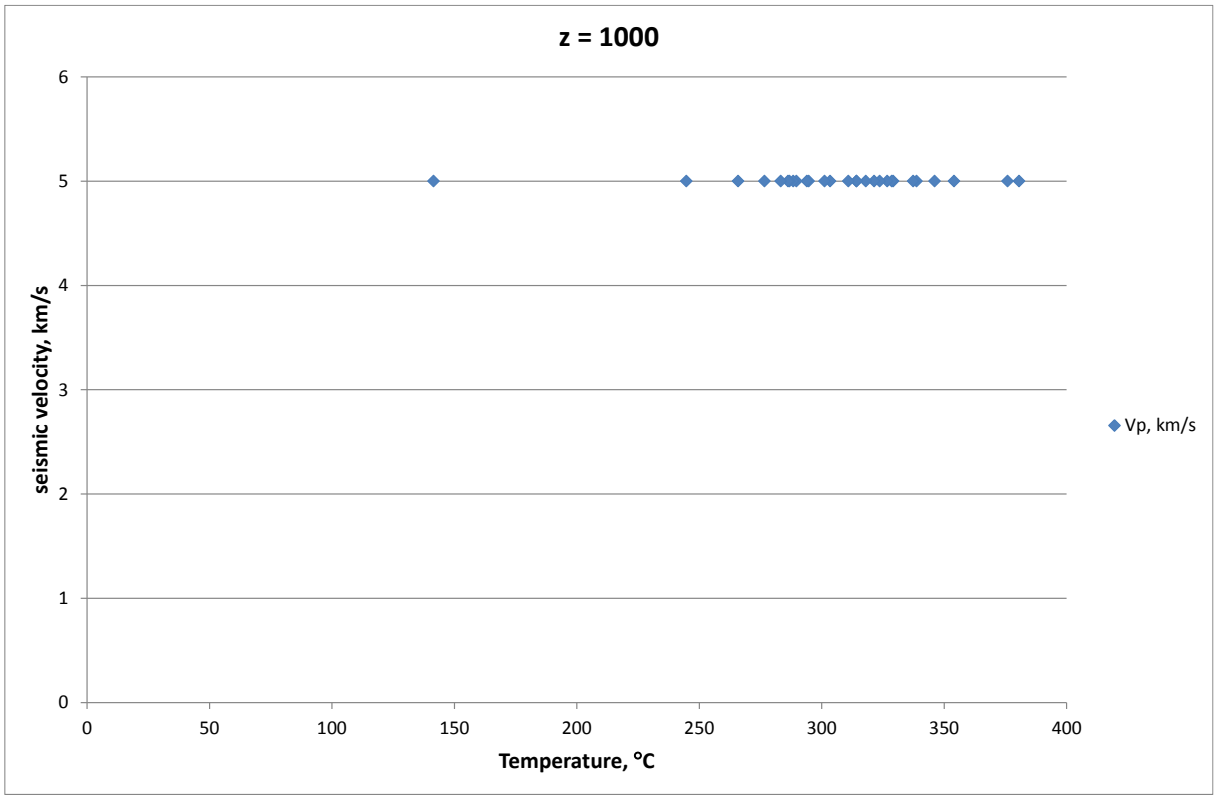

Figure 36: P-wave velocity as derived by the 1998 active seismic survey as a function of temperature at the same horizontal surface (z=1000 m asl), indicating no statistically significant relationship between the two parameters.

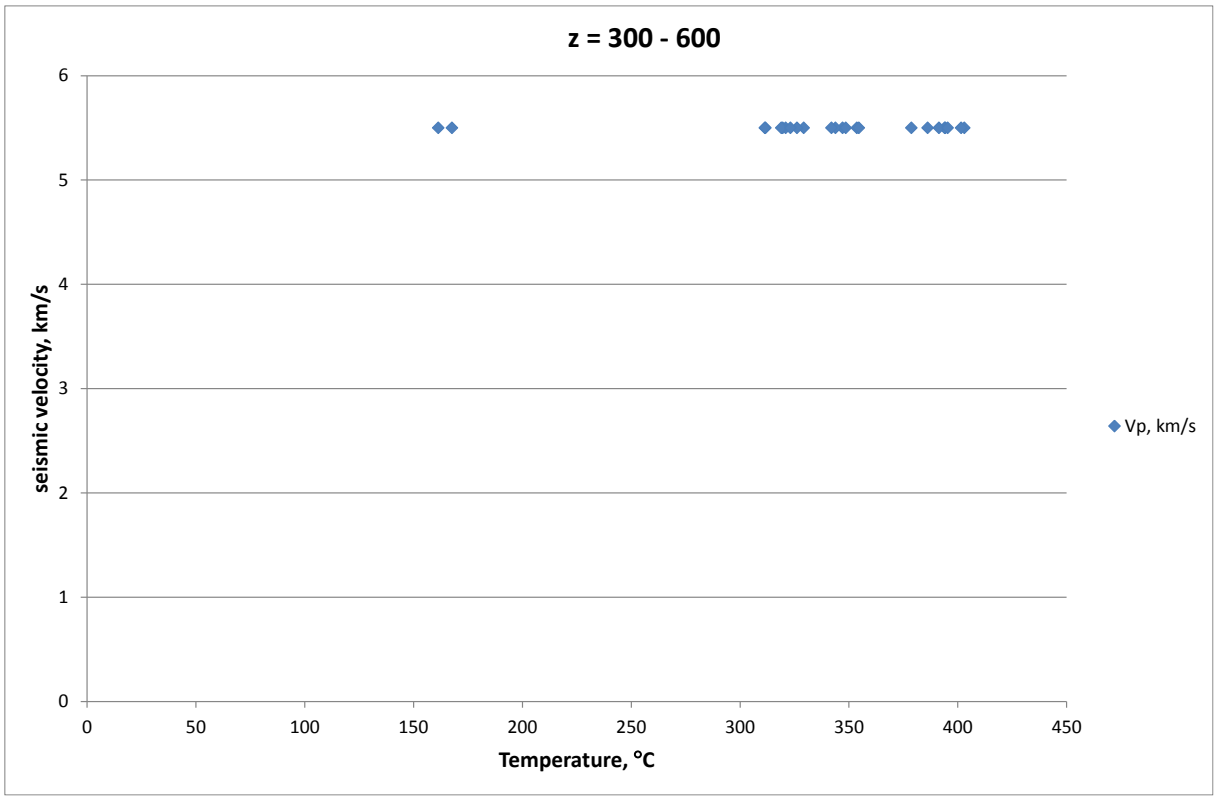

Figure 37: P-wave velocity as derived by the 1998 active seismic survey as a function of temperature at the same horizontal zone (z=300-600 m asl), indicating no statistically significant relationship between the two parameters.

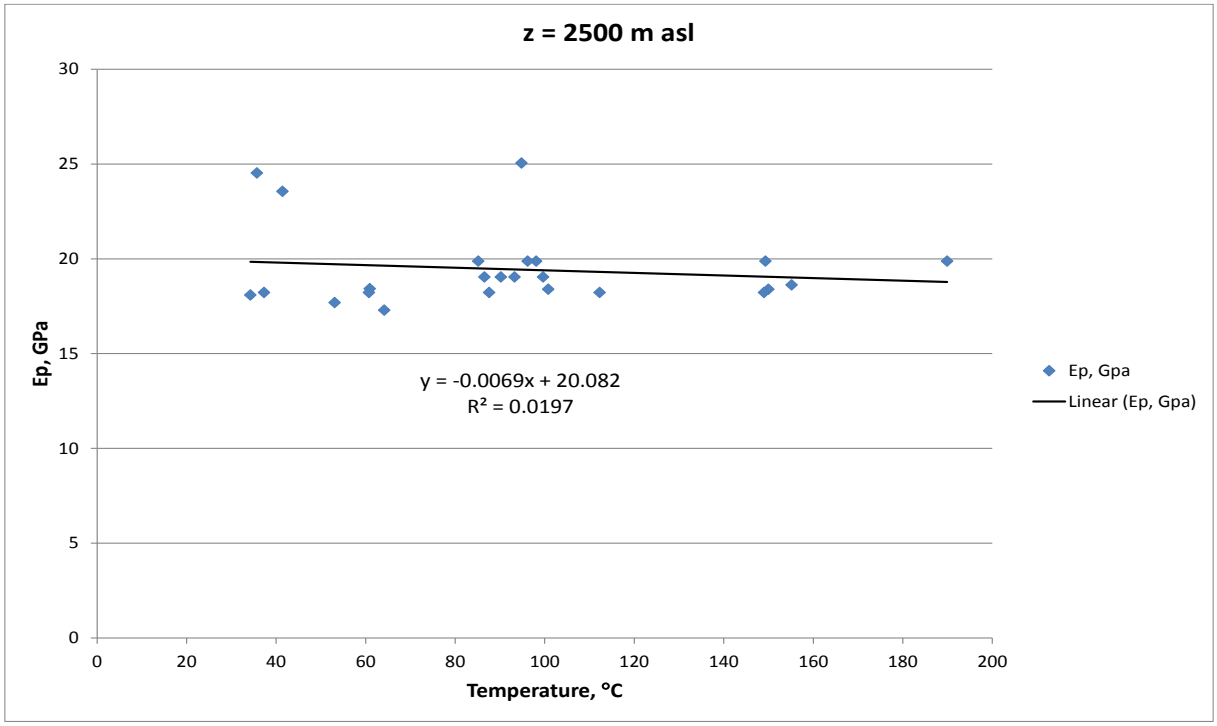

Figure 38: P-wave modulus as derived by the 1998 active seismic survey and regional density model as a function of temperature at the same horizontal surface (z=2500 m asl), indicating no statistically significant relationship between the two parameters.

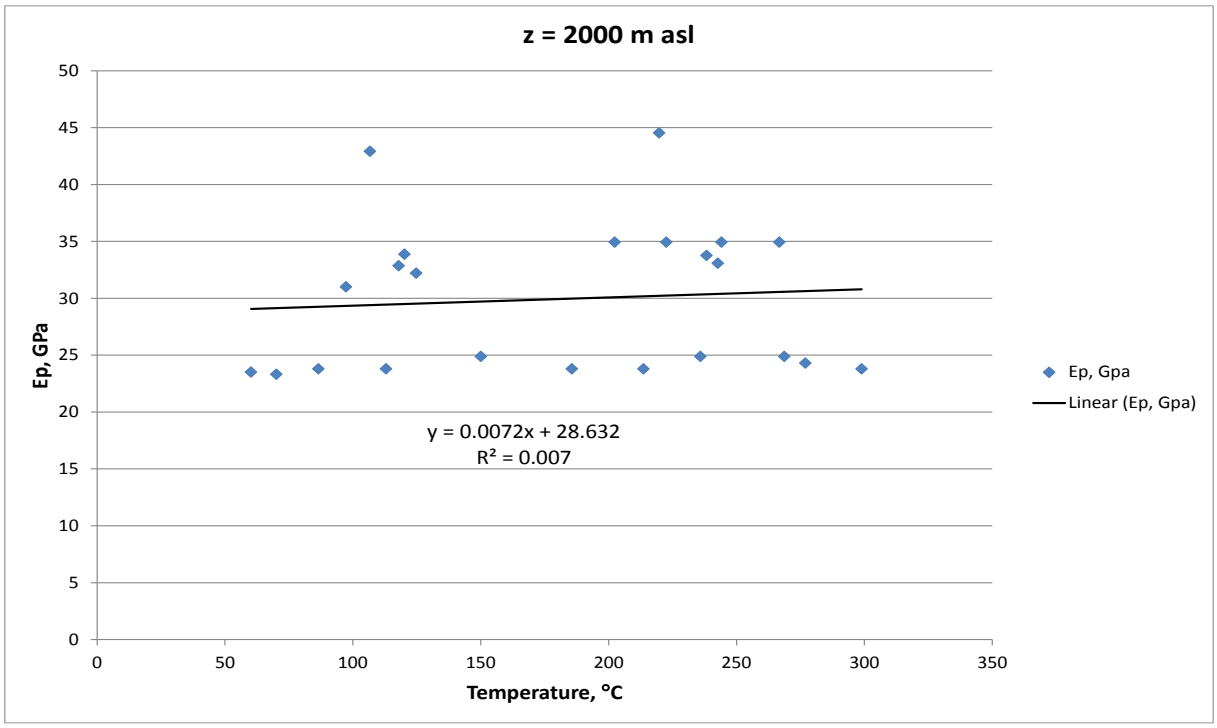

Figure 39: P-wave modulus as derived by the 1998 active seismic survey and regional density model as a function of temperature at the same horizontal surface (z=2000 m asl), indicating no statistically significant relationship between the two parameters.

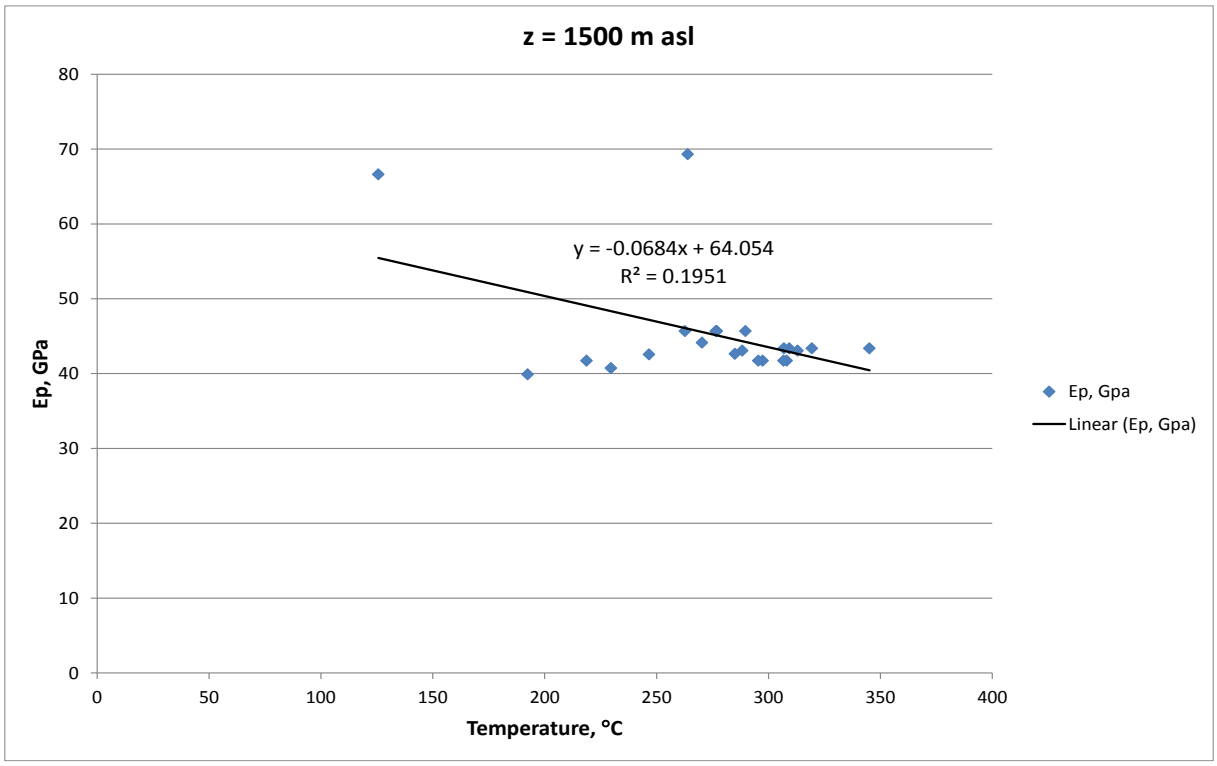

Figure 40: P-wave modulus as derived by the 1998 active seismic survey and regional density model as a function of temperature at the same horizontal surface (z=1500 m asl), indicating no statistically significant relationship between the two parameters.

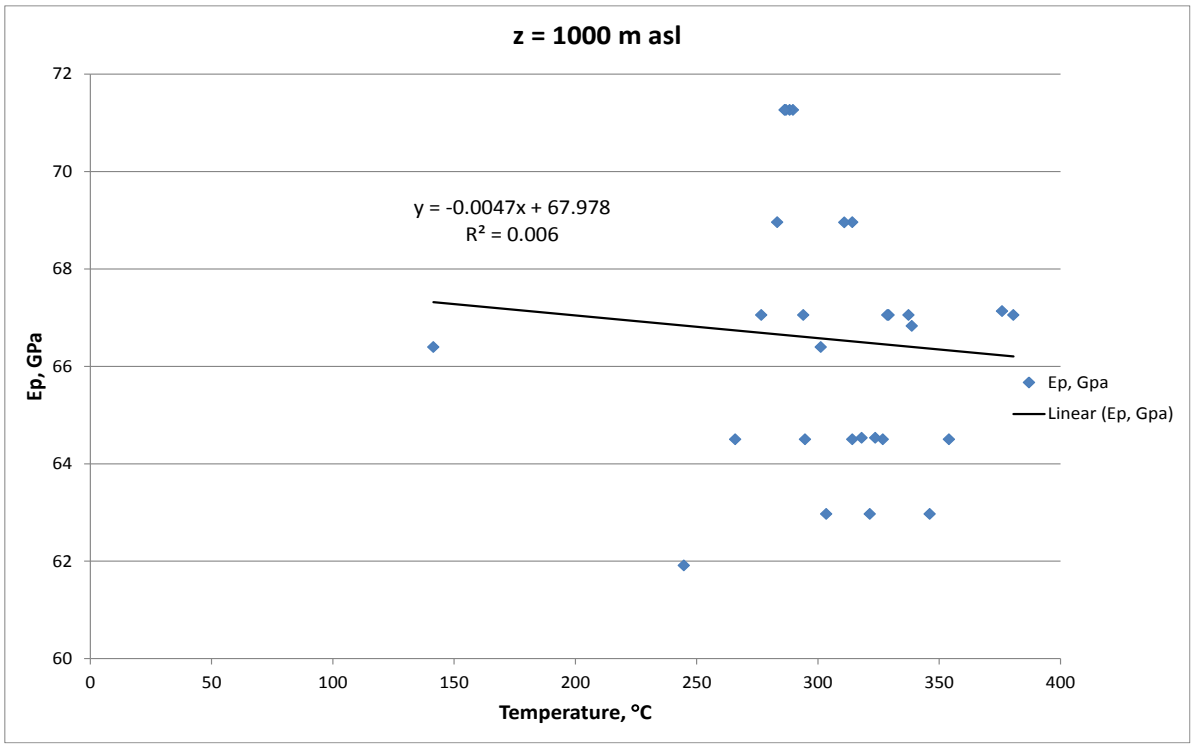

Figure 41: P-wave modulus as derived by the 1998 active seismic survey and regional density model as a function of temperature at the same horizontal surface (z=1000 m asl), indicating no statistically significant relationship between the two parameters.

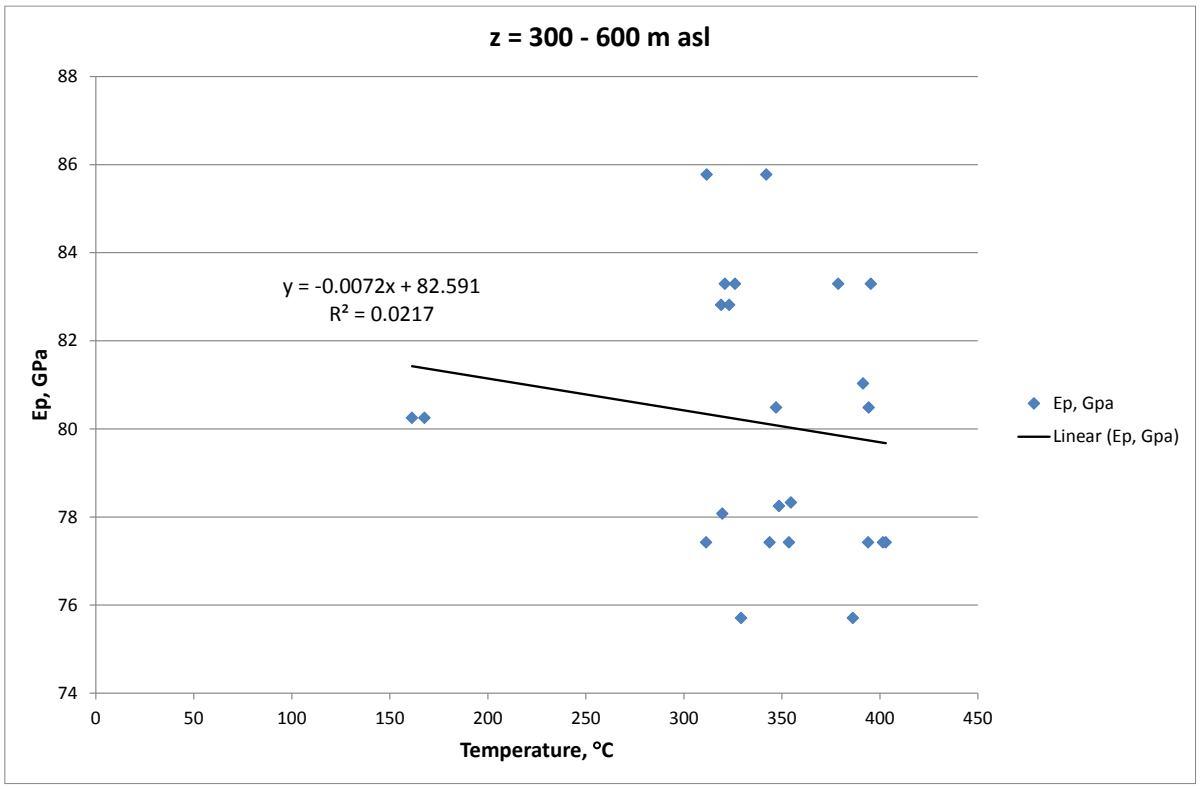

Figure 42: P-wave modulus as derived by the 1998 active seismic survey and regional density model as a function of temperature at the same horizontal zone (z=300-600 m asl), indicating no statistically significant relationship between the two parameters.

3.4 Multiple parameter linear regression analysis

For each one of the two seismic surveys performed in Los Humeros, a series of multiple linear regression analyses were run taking as independent variables temperature and elevation, or temperature and the logarithm of elevation and seeking potential correlations with one of the quantities P-wave velocity Vp, its logarithm Ln(Vp), S-wave velocity Vs, its logarithm Ln(Vs), P-wave modulus Ep, its logarithm Ln(Ep), S-wave modulus Es and its logarithm Ln(Es) as dependent variable. The SPSS package output of the analysis is presented in Annex 13.

The validity of specific assumptions was checked in each case, which are critical when performing multiple linear regression analysis in order to accept the derived correlations. These assumptions are linearity between each independent variable and the dependent variable, linearity between independent variables collectively and the dependent variable (by checking studentized residuals against the unstandardized predicted values), homoscedasticity, absence of multicollinearity and normality of the residuals. The results are presented in Annex 13 and are summarized in Table 3.2, where each line corresponds to one case.

Dependent variable	Independent variables	Year of Seismic Survey	Linearity between each independent variable and the dependent variable	Linearity between independent variables collectively and the dependent variable	Homoscedasticity	No multicollinearity	Normality of the residuals
Vp	T, Z	1998	⊘	⊘	⊘	✓	✓
Vp	T, Z	2018	⊘	⊘	⊘	✓	✓
Ln(Vp)	T, Z	1998	⊘	⊘	⊘	✓	✓
Ln(Vp)	T, Z	2018	⊘	⊘	⊘	✓	✓
Ln(Vp)	T, Ln(Z)	1998	⊘	⊘	⊘	✓	✓
Ln(Vp)	T, Ln(Z)	2018	⊘	⊘	⊘	✓	✓
Ep	T, Z	1998	⊘	⊘	⊘	✓	✓
Ep	T, Z	2018	⊘	⊘	⊘	✓	✓
Ln(Ep)	T, Z	1998	⊘	⊘	✓	✓	✓
Ln(Ep)	T, Z	2018	⊘	⊘	⊘	✓	✓
Ln(Ep)	T, Ln(Z)	1998	⊘	⊘	⊘	✓	✓
Ln(Ep)	T, Ln(Z)	2018	⊘	⊘	⊘	✓	✓
Vs	T, Z	2018	⊘	⊘	⊘	✓	✓
Ln(Vs)	T, Z	2018	⊘	⊘	⊘	✓	✓
Ln(Vs)	T, Ln(Z)	2018	⊘	⊘	⊘	✓	✓
Es	T, Z	2018	⊘	⊘	✓	✓	✓
Ln(Es)	T, Z	2018	⊘	⊘	⊘	✓	✓
Ln(Es)	T, Ln(Z)	2018	⊘	⊘	⊘	✓	✓

Table 3.2: Results of testing critical assumptions of multiple linear regression models with seismic velocity or elastic modulus as dependent variable and both temperature (T) and elevation (Z) as independent variables

In all cases, there was no linearity between each independent variable and the dependent variable, as assessed by partial regression plots, or linearity between independent variables collectively and the dependent variable, as assessed by a plot of studentized residuals against the predicted values for each case. With two exceptions, where the test was marginally passed, there was heteroscedasticity, as assessed by visual inspection of a plot of studentized residuals versus unstandardized predicted values.

On the other hand, the assumption of normality was met and there was no evidence of multicollinearity, as assessed by tolerance values greater than 0.1.

Therefore, assumptions met were the “no multicollinearity” and “normality of the results”, while assumptions not met were linearity (single and collective) and homoscedasticity. As all five assumptions must be met, in order to run a multiple linear regression model that provides valid results, we conclude that since the specific variables do not meet the required assumptions, we cannot properly examine if statistically significant relations occur between dependent variables Vp, Vs, Ep, Es, ln(Vp), ln(Vs), ln(Ep) and ln(Es) neither with T and Z, nor with T and ln(Z), on the basis of a multiple linear regression model.

In case of Vp as dependent variable and T and Z as independent variables, additional multiple linear regression analysis were run with all possible combinations of variables, their square, their square root and their logarithms, with the same results as above (“no multicollinearity” and “normality of the results” assumptions met, while “linearity” and “homoscedasticity” not).

3.5 Discussion

When examining the overall models dealing with the relation between T and Vp, Ep (for both 1998 and 2018 datasets), Vs and Es (only for 2018 dataset), the Compound, Growth, Exponential and Logistic Models seem to provide the best fit, on a statistical significant level, with the levels of R^2 varying around 70%.

When examining the overall models dealing with the relation between T and the centred and normalized values of Vp, Ep (for both 1998 and 2018 datasets), Vs and Es (only for 2018 dataset), no Models were identified to provide a good fit; in most cases, R^2 had a value lower than 5%. In addition, in many cases the model fitting results were not statistically significant (Sig. > 0,10).

When examining the individual models per well dealing with the relation between T and Vp, Ep (for both 1998 and 2018 datasets), Vs and Es (only for 2018 dataset), the Quadratic, Cubic, Compound, Growth, Exponential and Logistic Models seem to provide the best fit, on a statistical significant level. In the majority of the cases, the R^2 is higher than 90%; in only 2 wells (from the total 178 cases investigated) the R^2 has a value lower than 70% (but in any case, higher than 60%).

When examining the individual models per elevation level (Z) dealing with the relation between T and Vp, Ep (for both 1998 and 2018 datasets), Vs and Es (only for 2018 dataset), no Models were identified to provide a good fit; in most cases, R^2 had a value lower than 10%, while no model provided an $R^2 >$ 40%. In addition, in many cases the model fitting results were not statistically significant (Sig. > 0,10). Having in mind the general low R^2 values, it should be noted that the results of the models examining Vs and Es provided relatively higher R^2 values, compared to the ones dealing with Vp and Ep (this finding refers specifically to year 2018, as no data are available on Vs and Es for year 1998 dataset).

When examining the overall models dealing with the relation between Z and Vp, Ep (for both 1998 and 2018 datasets), Vs and Es (only for 2018 dataset), the Quadratic, Cubic, Compound, Growth, Exponential and Logistic Models seem to provide the best fit, on a statistical significant level. The Quadratic and cubic Models provide a R^2 of at least 90%, while the Compound, Growth, Exponential and Logistic Models provide a R^2 of at least 88%.

Inversion of the relationships presented in previous chapter in terms of temperature, is presented in Figures 43 and 44 for seismic velocities and Figures 45 and 46 for elastic moduli. The best fit logarithmic function to measured data points is presented in each case (T vs Vs/p and T vs Es/p), with the corresponding R^2 being slightly above 70%.

These logarithmic functions between temperature and seismic velocity or elastic moduli should be valid down to the point where maximum values of velocity or elastic moduli are observed. However, due to the weak correlations observed, it is uncertain whether these functions can be used for a reliable temperature prediction down to that point.

The fact that no statistically significant relationship between seismic velocities and elastic moduli was observed in the horizontal direction, suggests that the statistically significant correlation observed in the vertical direction corresponds to an indirect relation of seismic velocities and rock elastic moduli with temperature. For example, the strong and almost linear relationship of P-wave elastic modulus with elevation, points to a possible relationship with the lithostatic and/or pore pressure, while the

boiling point to depth pattern that is followed by temperature is based on a straight forward temperature relation with pore pressure. The influence of pore pressure on the elastic parameters should be considered in further investigation.

Local anisotropy is also important, as indicated by the scattering of the data points observed in Figures 43 to 46.

When examining the multiple linear regression assumptions with temperature (T) as dependent variable and seismic velocity or elastic modulus (Vp, or Vs, or Ep, or Es) and elevation (Z) as independent variables, including the logarithms of independent variables, which are presented in Annex 14 and summarized in Table 3.3, we observe no linearity with either each individual or both independent variables, but presence of homoscedasticity and residuals normality.

Moreover, in most cases of Z used as independent value, without any logarithmic transformation, the test of "no multicollinearity" is not passed, indicating a possible relation of Z with seismic velocities and elastic moduli. However, absence of multicollinearity is achieved when the logarithm of Z is used in the multiple linear regression analysis.

Dependent variable	Independent variables	Year of Seismic Survey	Linearity between each independent variable and the dependent variable	Linearity between independent variables collectively and the dependent variable	Homoscedasticity	No multicollinearity	Normality of the residuals
T	Vp, Z	1998	⊘	⊘	✓	⊘	✓
T	Vp, Z	2018	⊘	⊘	✓	⊘	✓
T	Vs, Z	2018	⊘	⊘	✓	⊘	✓
T	Ep, Z	1998	⊘	⊘	✓	✓	✓
T	Ep, Z	2018	⊘	⊘	✓	⊘	✓
T	Es, Z	2018	⊘	⊘	✓	⊘	✓
T	Ln(Vp), Z	1998	⊘	⊘	✓	⊘	✓
T	Ln(Vp), Z	2018	⊘	⊘	✓	⊘	✓
T	Ln(Vs), Z	2018	⊘	⊘	✓	⊘	✓
T	Ln(Ep), Z	1998	⊘	⊘	✓	✓	✓
T	Ln(Ep), Z	2018	⊘	⊘	✓	⊘	✓
T	Ln(Es), Z	2018	⊘	⊘	✓	✓	✓
T	Vp, Ln(Z)	1998	⊘	⊘	✓	✓	✓
T	Vp, Ln(Z)	2018	⊘	⊘	✓	✓	✓
T	Vs, Ln(Z)	2018	⊘	⊘	✓	✓	✓
T	Ep, Ln(Z)	1998	⊘	⊘	✓	✓	✓
T	Ep, Ln(Z)	2018	⊘	⊘	✓	✓	✓
T	Es, Ln(Z)	2018	⊘	⊘	✓	✓	✓
T	Ln(Vp), Ln(Z)	1998	⊘	⊘	✓	✓	✓
T	Ln(Vp), Ln(Z)	2018	⊘	⊘	✓	✓	✓
T	Ln(Vs), Ln(Z)	2018	⊘	⊘	✓	✓	✓
T	Ln(Ep), Ln(Z)	1998	⊘	⊘	✓	✓	✓
T	Ln(Ep), Ln(Z)	2018	⊘	⊘	✓	✓	✓
T	Ln(Es), Ln(Z)	2018	⊘	⊘	✓	✓	✓

Table 3.3: Results of tested assumptions of multiple linear regression models with temperature (T) as dependent variable and seismic velocity or elastic modulus (Vp, or Vs, or Ep, or Es) and elevation (Z) as independent variables

Even though we cannot properly examine if statistically significant linear relations occur (as required assumptions are not met) between T and the seismic velocities or elastic moduli and elevation, further nonlinear models could be investigated.

This analysis has been performed utilising elastic seismic quantities, which produces results independent from seismic frequency. In the deepest part of volcanic geothermal systems however and close to the heat source, seismic parameters have typically inelastic behaviour, as shown in the annexes of GEMex deliverable D5.5 and in Poletto et al. (2018) and Farina et al. (2019). In this case, when inelasticity is included in the analysis, results dependent on the seismic frequency could be expected. We consider that this aspect can be subject to further investigations.

In order to define rock and fluid physical properties (pressure, temperature, etc.) at the deeper part of the Los Humeros geothermal system and investigate their relation with seismic parameters and rock moduli, drilling, logging and testing of a new deep well at least down to 5 km depth is necessary.

The fact that different correlations have been derived between temperature and P-wave velocity and modulus during the legacy active survey of 1998 and the new passive survey of 2018, could be attributed to the different timing of the two surveys by 20 years. During these 20 years the seismic properties of the subsurface may have been changed due to the withdrawal of large fluid quantities from the production wells, which have affected field wise the subsurface pore pressure distribution and in the close vicinity of the production and reinjection wells the temperature regime.

A set of new P-T logs within all Los Humeros wells, will provide the necessary updated data of subsurface pore pressure and temperature distribution, which should be input to a further multiple parameter statistical analysis, correlating seismic velocities and elastic properties with temperature, lithostatic pressure and pore pressure.

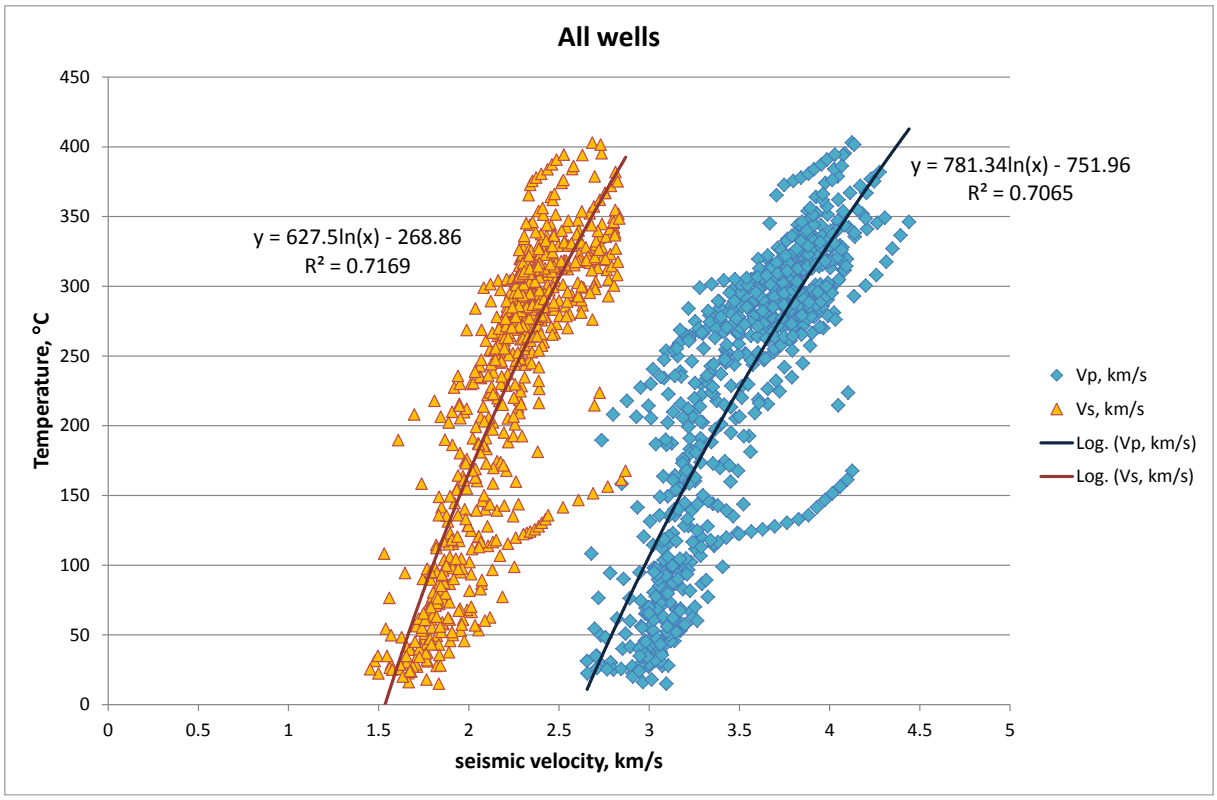

Figure 43: Measured temperature as a function of seismic velocities as derived by passive seismic survey in Los Humeros and best fit logarithmic functions.

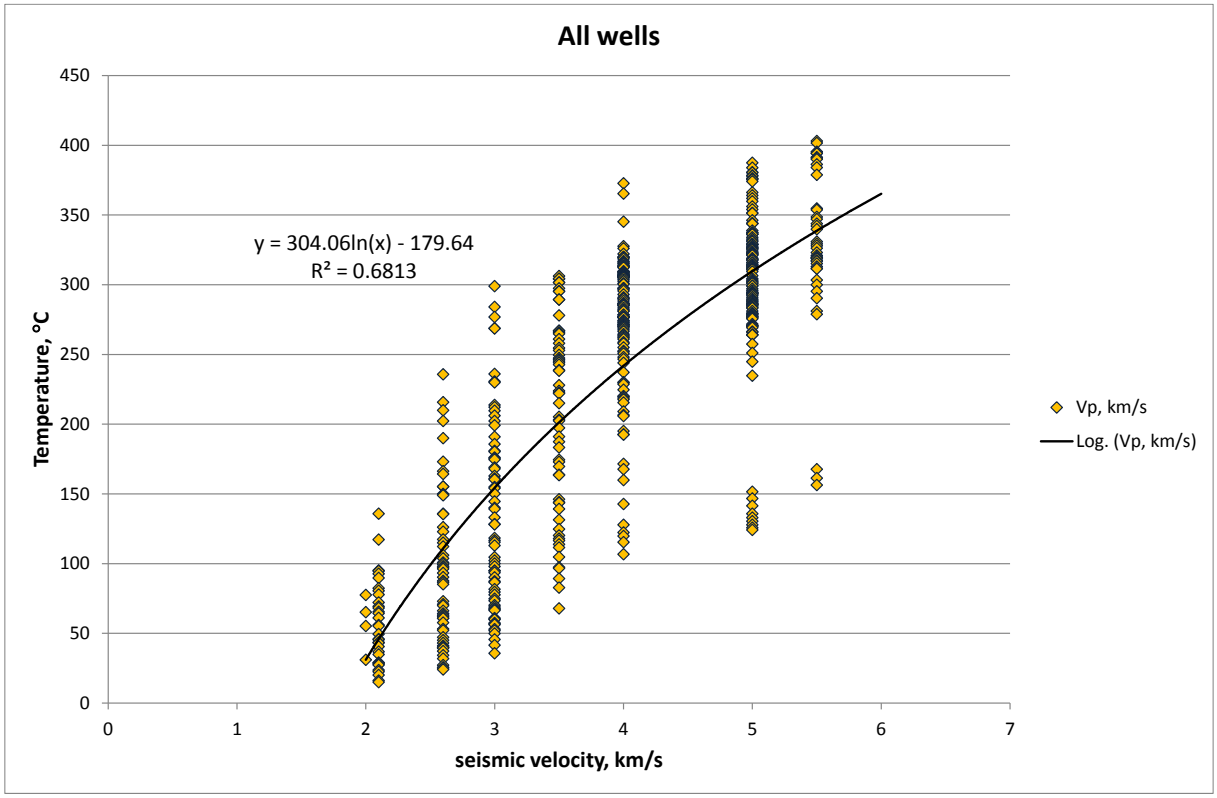

Figure 44: Measured temperature as a function of seismic velocities as derived by past active seismic survey in Los Humeros and best fit logarithmic functions.

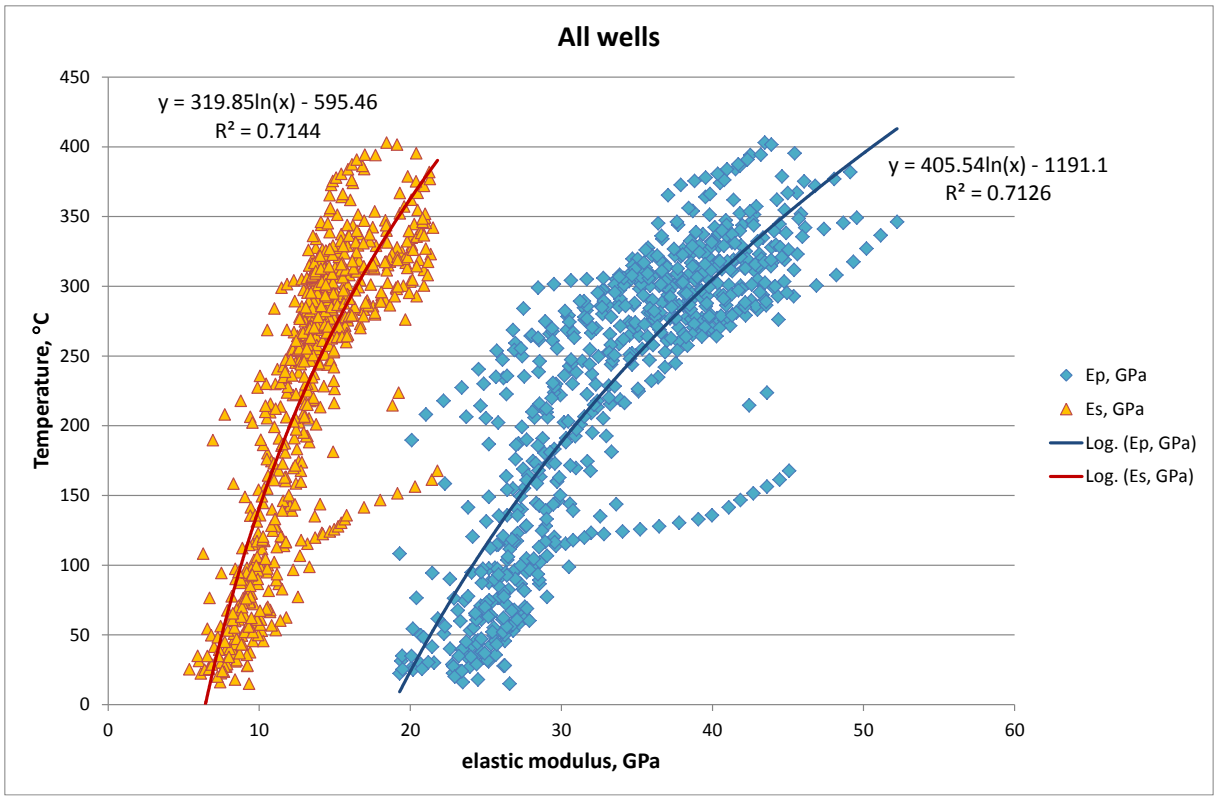

Figure 45: Measured temperature as a function of elastic moduli as derived by passive seismic and regional gravity surveys in Los Humeros and best fit logarithmic functions.

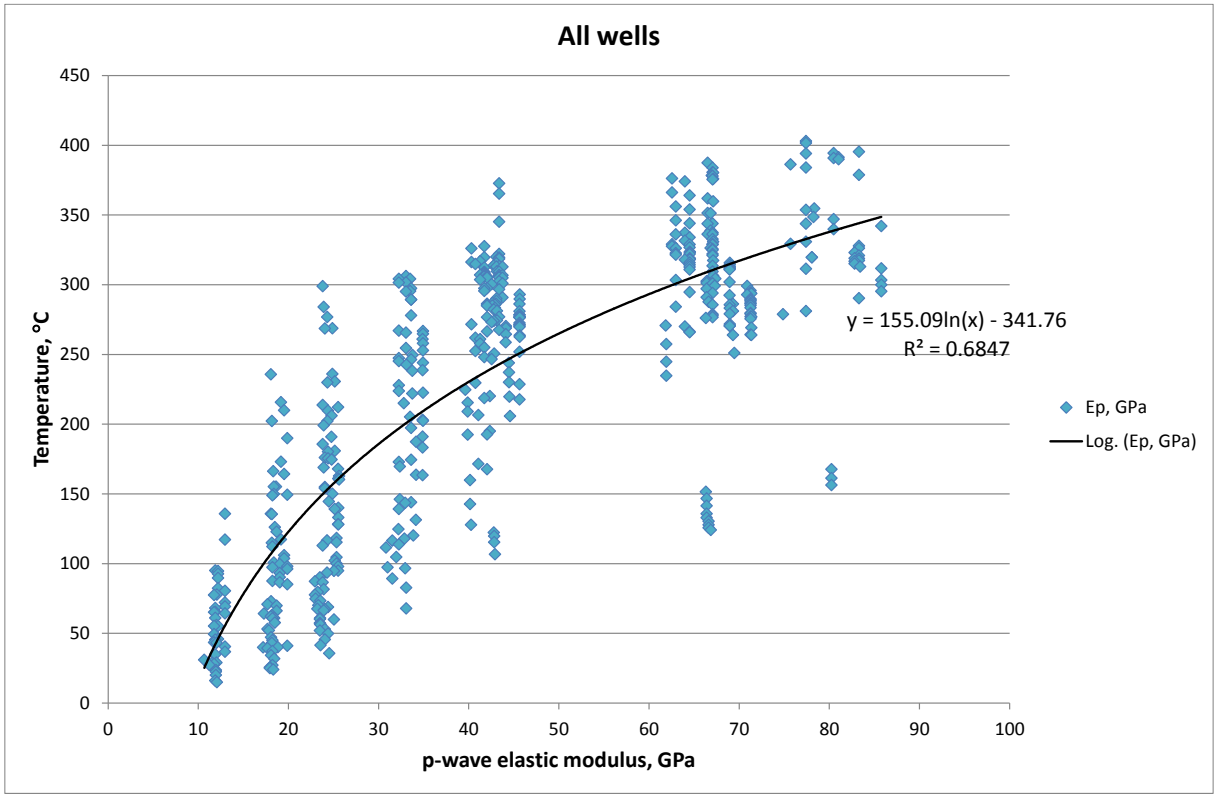

Figure 46: Measured temperature as a function of elastic moduli as derived by past active seismic and regional gravity surveys in Los Humeros and best fit logarithmic functions.

4 Conclusion

Both Acoculco (EGS) and Los Humeros (superhot) are high-elevation geothermal systems with wellheads located at 2700-2800 m asl altitude.

In Acoculco, the temperature increases linearly with depth down to well bottom, which is located at 800 m asl elevation, trend typical of conductive geothermal systems of almost zero permeability. 1-D S-wave modulus values, derived from ambient seismic noise and gravity surveys carried out in the field, indicate that S-wave formation modulus increases with depth down to around 0 m asl elevation, where a local maximum value is observed.

In Acoculco, a statistically significant correlation exists between 1-D S-wave modulus and temperature, which corresponds to second order polynomial or logarithmic functions down to 0 m asl.

In Los Humeros, the temperature down to -300 m asl increases with depth approaching the boiling point to depth model, which is typical for convective hydrothermal systems of high permeability, including the upper part of a superhot convective system. The P-wave formation modulus of elasticity, as derived from past active seismic and recent 3-D passive seismic surveys, increases more or less with depth, with minor horizontal variations. The S-wave formation modulus, as derived by 1-D ambient seismic noise and past active seismic and recent 3-D passive seismic surveys increases with depth down to elevation level of around 500 m asl, also depending on location, and remains approximately constant at deeper levels. Variation in the horizontal direction is more pronounced in S-wave elastic modulus than in P-wave one.

In Los Humeros, a weak statistically significant relation exists between both P-wave and S-wave elastic moduli with temperature in the vertical direction, which can be expressed as exponential and second order polynomial functions. No such statistically significant correlation is evident in the horizontal direction.

Further research in this direction should include the field investigation of seismic properties and rock moduli and their relation to pressure and temperature at both the upper 3 km of Los Humeros where rock behaves as an elastic medium, and at the deeper part of the system where inelasticity prevails, seismic frequency becomes important and variations of seismic velocities and rock moduli with temperature are sharp.

5 Acknowledgements

The Federal Electricity Commission of Mexico (CFE) is acknowledged for the data they provided from measurements within their wells in Los Humeros and Acoculco geothermal fields and for the raw data of the legacy active seismic survey carried out in Los Humeros in 1998.

In addition, the following European and Mexican partners of the GEMex consortium are acknowledged:

- Dr. Philippe Jousset and Dr. Tania Andrea Toledo Zambrano (GFZ-Potsdam) for the 1-D and 3-D seismic velocity models of Los Humeros obtained from the passive seismic survey of 2018.
- Dr. Katrin Loeer (HS-Bochum) for her 1-D shear wave velocity profile of Los Humeros obtained from ambient seismic noise analysis.
- Dr. Rosa Maria Prol Ledesma and Dr. Marco Calo (UNAM) for the 1-D seismic velocity model of Acoculco obtained from ambient seismic noise analysis.
- Dr. Eva Schill and Dr. Natalia Cornejo (KIT) for the density profiles at Acoculco and selected Los Humeros wells from their local density models.
- Dr. Marco A. Perez and Dr. Jonathan Carrillo Lopez, (CICESE) for the 3D regional density model of Los Humeros.
- Dr. Paromita Deb (RWTH-Aachen) for the simulated temperatures by her reservoir models at Acoculco and selected Los Humeros wells.
- Dr. Damien Bonte (U. of Utrecht) for the maximum recorded temperatures and his static temperature projections using the Horner method.

6 List of Annexes

(Confidential, provided as separate documents)

Annex I: LOS HUMEROS: EVALUATION OF P-T LOGS

Annex II: ACOCULCO: EVALUATION OF P-T LOGS

Annex III: LOS HUMEROS: SUBSURFACE TEMPERATURE DISTRIBUTION

Annex IV: LOS HUMEROS: SUBSURFACE DISTRIBUTION OF ROCK MODULI Ep, Es

Annex V: REFLECTION SEISMIC SURVEY IN LOS HUMEROS: SEISMIC VELOCITY Vp, ROCK MODULUS Ep AND CORRELATION WITH TEMPERATURE AT WELL LOCATIONS

Annex VI: STATISTICAL ANALYSIS; REFLECTION (1998) AND PASSIVE (2018) SEISMIC SURVEYS IN LOS HUMEROS; CURVE FITTING OF SEISMIC VELOCITIES Vp and Vs AS A FUNCTION OF TEMPERATURE AT WELL LOCATIONS

Annex VII: STATISTICAL ANALYSIS; REFLECTION (1998) AND PASSIVE (2018) SEISMIC SURVEYS IN LOS HUMEROS; CURVE FITTING OF ELASTIC MODULI Ep and Es AS A FUNCTION OF TEMPERATURE AT WELL LOCATIONS

Annex VIII: STATISTICAL ANALYSIS; REFLECTION (1998) AND PASSIVE (2018) SEISMIC SURVEYS IN LOS HUMEROS; CURVE FITTING OF SEISMIC VELOCITIES Vp and Vs AS A FUNCTION OF TEMPERATURE AT HORIZONTAL LEVELS

Annex IX: STATISTICAL ANALYSIS; REFLECTION (1998) AND PASSIVE (2018) SEISMIC SURVEYS IN LOS HUMEROS; CURVE FITTING OF ELASTIC MODULI Ep and Es AS A FUNCTION OF TEMPERATURE AT HORIZONTAL LEVELS

Annex X: STATISTICAL ANALYSIS; REFLECTION (1998) AND PASSIVE (2018) SEISMIC SURVEYS IN LOS HUMEROS; CURVE FITTING OF SEISMIC VELOCITIES Vp and Vs AND ELASTIC MODULI Ep and Es AS A FUNCTION OF TEMPERATURE

Annex XI: STATISTICAL ANALYSIS; REFLECTION (1998) AND PASSIVE (2018) SEISMIC SURVEYS IN LOS HUMEROS; CURVE FITTING OF SEISMIC VELOCITIES Vp and Vs AND ELASTIC MODULI Ep and Es AS A FUNCTION OF ELEVATION

Annex XII: STATISTICAL ANALYSIS; REFLECTION (1998) AND PASSIVE (2018) SEISMIC SURVEYS IN LOS HUMEROS; CURVE FITTING OF NORMALIZED SEISMIC VELOCITIES AND NORMALIZED ELASTIC MODULI AS A FUNCTION OF TEMPERATURE

Annex XIII: STATISTICAL ANALYSIS; REFLECTION (1998) AND PASSIVE (2018) SEISMIC SURVEYS IN LOS HUMEROS; MULTIPLE REGRESSION ANALYSIS OF SEISMIC VELOCITIES VP OR VS OR ELASTIC MODULI EP OR ES AS A FUNCTION OF TEMPERATURE AND ELEVATION

Annex XIV: STATISTICAL ANALYSIS; REFLECTION (1998) AND PASSIVE (2018) SEISMIC SURVEYS IN LOS HUMEROS; MULTIPLE REGRESSION ANALYSIS OF TEMPERATURE AS A FUNCTION OF SEISMIC VELOCITIES VP OR VS OR ELASTIC MODULI EP OR ES AND ELEVATION.

7 References

Bonté, D., Limberger, J., Trumpy, E., Gola, G., van Wees, J.D. (2019). GEMex deliverable D3.4 "Regional resource assessment and geothermal models"

Calcagno, Ph., Evanno, G., Trumpy, E., Gutiérrez-Negrín, L.C., Macías, J.L., Carrasco-Núñez, G., and Liotta, D. (2018): Preliminary 3-D geological models of Los Humeros and Acoculco geothermal fields (Mexico) – H2020 GEMex Project.

Calo, M. (2019): 1-D seismic velocity model of Acoculco provided by the Mexican partners (Instituto de Geofísica, UNAM, PT5.2 SISMICA) calculated using ambient noise analysis.

CFE: P-T (Pressure and Temperature) logs in wells EAC-1 and EAC-2 in Acoculco

CFE: P-T (Pressure and Temperature) logs in 52 wells in Los Humeros

CFE (1998): Raw data of the legacy active seismic survey

Deb, P., Knapp, D., Marquart, G., Clauser, C. (2019a). GEMex deliverable D6.2 "Report on the numerical reservoir model used for the simulation of the Acoculco reservoir in Mexico"

Deb, P., Knapp, D., Marquart, G., Clauser, C. (2019b). GEMex deliverable D6.3 "Report on the numerical reservoir model used for the simulation of the Los Humeros super-hot reservoir in Mexico"

Farina, B., Poletto, F., Mendrinos, D., Carcione, J.M., Karytsas C. (2019). Seismic properties in conductive and convective hot and super-hot geothermal systems. Geothermics 82, 16–33.

Gutiérrez, A.G. (2009), "Estado térmico inicial del campo geotérmico de Los Humeros, Puebla, México", Geotermia, Vol. 22, No.1, Enero-Junio de 2009 (in Spanish)

Jousset, Ph., and Agustsson, K., Barison, E., Böhm, G., Boullenger, B., Caló, M., Chavarria, I.G., Farina, B., Gaucher, E., Loeer, K., Martins, J., Perton, M., Poletto, F., Saenger, E., Soto, A.F., Toledo, T., Verdel, A., Werner, C. (2019). GEMex Deliverable D5.3 "Seismic structures of the Acoculco and Los Humeros geothermal fields", chapters 5.4 and 5.7.

Liu, Z.L., Dong, X.F., Liu, Z.T., & Liu, Q.H. (Eds.). (2013). Environmental Protection and Resources Exploitation. Trans Tech Publications Ltd. pp 776.

Loeer, K., Riahi, N., Saenger, E.H. (2019): "Investigating the deep structures of the Los Humeros geothermal field, Mexico, with three-component beamforming of ambient seismic noise", Geophysical Research Abstracts, Vol. 21, EGU2019-PREVIEW, 2019, EGU General Assembly 2019.

Perez, M.A. and Lopez J.C. (2019): 3D regional density model from Los Humeros provided by the Mexican partners (CICESE, Earth Sciences Division) calculated from gravity survey.

Poletto, F., Farina, B., Carcione, J.M. (2018). Sensitivity of seismic properties to temperature variations in a geothermal reservoir. Geothermics 76, 149–163.

Poletto, F., Farina, B., Carcione, J.M., Böhm, G., Mendrinos, D., Jousset, Ph., Pinna, G., Barison, E. (2019). GEMex Deliverable D5.5 “Report on seismic modelling”

Schill, E., Cornejo, N. (2019). GEMex deliverable D5.6 “Gravity modelling”.

Toledo, T., Gaucher, E., Metz, M., Jousset, Ph., Maurer, H., Krawczyk, C., Figueroa, A. and Calo, M. (2019): “Seismic earthquake tomography imaging of the Los Humeros geothermal field, Mexico: first results”, Geophysical Research Abstracts, Vol. 21, EGU2019-15960-1, 2019, EGU General Assembly 2019.

Toledo, T.; Gaucher, E.; Metz, M.; Calò, M.; Figueroa, A.; Angulo, J.; Jousset, P.; Kieling, K.; Saenger, E (2019): Dataset of the 6G seismic network at Los Humeros, 2017-2018. GFZ Data Services. Other/Seismic Network. doi:10.14470/1T7562235078.

Coordination Office, GEMex project

Helmholtz-Zentrum Potsdam
Deutsches GeoForschungsZentrum

Telegrafenberg, 14473 Potsdam

Germany